# Applications of Electrochemical Impedance Spectroscopy to Hydrogen Adsorption, Evolution and Absorption into Metals

Andrzej Lasia

Département de chimie, Université de Sherbrooke, Sherbrooke, Québec, J1K 2R1 Canada

## I. INTRODUCTION

In the first part of this review[1] we have presented fundamental aspects of electrochemical impedance spectroscopy (EIS) and showed how they can be used in data validation and modeling of processes limited by diffusion, electrode kinetics and adsorption for cases of different types of electrode geometries. In this chapter we shall present a general matrix method for impedance determination and apply it to solve electrochemical problems connected with H adsorption and absorption, and evolution of $H_2$. These processes present many problems which are similar to those found in metal underpotential deposition, intercalation, corrosion, etc. Of course, the literature of this subject is very rich and only some selected applications, which illustrate development of various typical impedances, will be presented. Obviously, it is assumed that the impedance was correctly measured and validated. This presentation should help researchers to develop equations for impedances and transfer functions, and correctly model

1

the electrode processes to which they are applied. This is the most difficult, but quickly developing, part of the whole field. With a good knowledge of the literature, it is possible to avoid many pitfalls of electrochemical impedance spectroscopy (EIS). It should be stressed again that EIS is a very sensitive technique but it is usually not sufficient to solve all the emergent problems. Good transfer of knowledge from other electro-chemical and nonelectrochemical techniques is a complementary requirement.

## II. DETERMINATION OF IMPEDANCES

Impedances may be written for any mechanism. The use of matrix notation simplifies complex calculations. Below, a general method using matrices is presented and applied to a complex mechanism. This method will be used throughout this chapter.

Let us suppose that species A and C are soluble (diffusing species) and species B is adsorbed on the electrode surface:

$$A + e \rightleftarrows B_{ads} \tag{1}$$

$$B_{ads} + e \rightleftarrows C \tag{2}$$

Rates of these processes may be described by the following equations:

$$v_1 = \vec{k}_1 c_A(0)(1 - \Theta) - \overleftarrow{k}_{-1}\Theta \tag{3a}$$
$$v_2 = \vec{k}_2 \Theta - \overleftarrow{k}_{-2}(1 - \Theta)c_C(0) \tag{3a}$$

where subscripts 1 and 2 correspond to reactions (1) and (2), $\Theta$ is the fractional surface coverage by B, that is the ratio of the surface concentration of B, $\Gamma_B$, to the maximal surface concentration, $\Gamma_\infty$, $\vec{k}_i = k_i \exp(-\beta fE)$ and $\overleftarrow{k}_{-i} = k_{-i} \exp[(1-\beta)fE]$ are the potential-dependent rates of these reactions, $\beta$ is the symmetry coefficient, $\eta$ the overpotential, and $C_A(0)$ and $C_C(0)$ are surface concentrations of the

soluble species A and C. From the equilibrium condition ($v_1 = v_2 = 0$) arises the following well-known relation between rate constants and concentrations:

$$\frac{k_1 k_2}{k_{-1} k_{-2}} \frac{C_A^*}{C_C^*} = 1 \tag{4}$$

where $C_A^*$ and $C_C^*$ are the bulk concentrations of species A and C.

In order to solve the problem described by Eqs. (1)-(2) it is necessary to write equations for: (i) current as a function of the rate constants, Eq. (7) below, (ii) current as function of fluxes of diffusing species, Eq. (6), and (iii) the mass balance relations for adsorbed species, Eq. (9). The total current flowing in a steady-state is given as:

$$i = 2FD_A \left( \frac{\partial C_A}{\partial x} \right)_{x=0} = -2FD_C \left( \frac{\partial C_C}{\partial x} \right)_{x=0}$$
$$= F(v_1 + v_2) = Fr_0 \tag{5}$$

Where $r_0 = v_1 + v_2$. Next, these equations must be written for phasors. Assuming linear, semi-infinite, diffusion, the oscillating current may be written (see Part I, Section III.2, ref. 1) as

$$\tilde{i} = -2F\sqrt{j\omega D_A}\, \tilde{C}_A(0) = 2F\sqrt{j\omega D_C}\, \tilde{C}_C(0) \tag{6}$$

and

$$\tilde{i} = F\tilde{r}_0 = F\left[ \left( \frac{\partial r_0}{\partial \eta} \right)\tilde{\eta} + \left( \frac{\partial r_0}{\partial \Theta} \right)\tilde{\Theta} + \left( \frac{\partial r_0}{\partial C_A} \right)\tilde{C}_A(0) + \left( \frac{\partial r_0}{\partial C_C} \right)\tilde{C}_C(0) \right] \tag{7}$$

Moreover, the mass balance for adsorbed species must be added, i.e.

$$\Gamma_\infty \frac{d\Theta_B}{dt} = v_1 - v_2 = r_1 \tag{8}$$

where $r_1 = v_1 - v_2$ is the rate of adsorption of B. Equation (8), written for phasors, is:

$$\Gamma_\infty j\omega\tilde{\Theta} = \left(\frac{\partial r_1}{\partial \eta}\right)\tilde{\eta} + \left(\frac{\partial r_1}{\partial \Theta}\right)\tilde{\Theta} + \left(\frac{\partial r_1}{\partial C_A}\right)\tilde{C}_A(0) + \left(\frac{\partial r_1}{\partial C_C}\right)\tilde{C}_C(0) \tag{9}$$

Equations (6), (7) and (8) may be rearranged into:

$$\frac{\tilde{i}}{F} = \left(\frac{\partial r_0}{\partial \eta}\right)\tilde{\eta} + \left(\frac{\partial r_0}{\partial \Theta}\right)\tilde{\Theta} + \left(\frac{\partial r_0}{\partial C_A}\right)\tilde{C}_A(0) + \left(\frac{\partial r_0}{\partial C_C}\right)\tilde{C}_C(0)$$

$$\frac{\tilde{i}}{2F} = -\sqrt{j\omega D_A}\tilde{C}_A(0)$$

$$\frac{\tilde{i}}{2F} = \sqrt{j\omega D_C}\tilde{C}_C(0) \tag{10}$$

$$\Gamma_\infty j\omega\tilde{\Theta} = \left(\frac{\partial r_1}{\partial \eta}\right)\tilde{\eta} + \left(\frac{\partial r_1}{\partial \Theta}\right)\tilde{\Theta} + \left(\frac{\partial r_1}{\partial C_A}\right)\tilde{C}_A(0) + \left(\frac{\partial r_1}{\partial C_C}\right)\tilde{C}_C(0)$$

or, in a matrix form $\mathbf{Y = AX}$, after division by $\tilde{\eta}$:

$$
\begin{bmatrix}
-\dfrac{\partial r_{0,\eta}}{\partial \eta} \\[2mm]
0 \\[2mm]
0 \\[2mm]
-\dfrac{\partial r_1}{\partial \eta}
\end{bmatrix}
=
\begin{bmatrix}
-\dfrac{1}{F} & \dfrac{\partial r_0}{\partial \Theta} & \dfrac{\partial r_0}{\partial C_A} & \dfrac{\partial r_0}{\partial C_C} \\[3mm]
-\dfrac{1}{2F} & 0 & -\sqrt{j\omega D_A} & 0 \\[3mm]
-\dfrac{1}{2F} & 0 & 0 & \sqrt{j\omega D_C} \\[3mm]
0 & \dfrac{\partial r_1}{\partial \Theta} - \Gamma_\infty j\omega & \dfrac{\partial r_1}{\partial C_A} & \dfrac{\partial r_1}{\partial C_C}
\end{bmatrix}
\begin{bmatrix}
\dfrac{\tilde{i}}{\tilde{\eta}} \\[3mm]
\dfrac{\tilde{\Theta}}{\tilde{\eta}} \\[3mm]
\dfrac{\tilde{C}_C(0)}{\tilde{\eta}} \\[3mm]
\dfrac{\tilde{C}_A(0)}{\tilde{\eta}}
\end{bmatrix}
\tag{11}
$$

The Faradaic admittance is $\tilde{Y}_f = -\tilde{i}/\tilde{\eta}$ and may be calculated using Cramer's rule: $\hat{Y}_f = -T/B$, where $B$ is the determinant of $\mathbf{A}$, and

determinant $T$ is obtained by substitution of the first column in $B$ by $Y = \det(\mathbf{Y})$:

$$T = \begin{vmatrix} -\dfrac{\partial r_0}{\partial \eta} & \dfrac{\partial r_0}{\partial \Theta} & \dfrac{\partial r_0}{\partial C_A} & \dfrac{\partial r_0}{\partial C_C} \\[2mm] 0 & 0 & -\sqrt{j\omega D_A} & 0 \\[2mm] 0 & 0 & 0 & \sqrt{j\omega D_C} \\[2mm] -\dfrac{\partial r_1}{\partial \eta} & \dfrac{\partial r_1}{\partial \Theta} - \Gamma_\infty j\omega & \dfrac{\partial r_1}{\partial C_A} & \dfrac{\partial r_1}{\partial C_C} \end{vmatrix} \qquad (12a)$$

and

$$B = \begin{vmatrix} -\dfrac{1}{F} & \dfrac{\partial r_0}{\partial \Theta} & \dfrac{\partial r_0}{\partial C_A} & \dfrac{\partial r_0}{\partial C_C} \\[2mm] -\dfrac{1}{2F} & 0 & -\sqrt{j\omega D_A} & 0 \\[2mm] -\dfrac{1}{2F} & 0 & 0 & \sqrt{j\omega D_C} \\[2mm] 0 & \dfrac{\partial r_1}{\partial \Theta} - \Gamma_\infty j\omega & \dfrac{\partial r_1}{\partial C_A} & \dfrac{\partial r_1}{\partial C_C} \end{vmatrix} \qquad (12a)$$

These determinants may be expanded into:

$$\begin{aligned} T &= \sqrt{D_A D_C}\left[ -\Gamma_\infty r_{0,\eta}(j\omega)^2 + \left( r_{0,\eta} r_{1,\Theta} - r_{0,\Theta} r_{1,\eta} \right)(j\omega) \right] \\ &= a_4 (j\omega)^2 + a_2 (j\omega) \end{aligned} \qquad (13a)$$

$$B = \frac{1}{2F}\begin{bmatrix} -2\sqrt{D_A D_C}\,\Gamma_\infty (j\omega)^2 \\ +\Gamma_\infty\left(-\sqrt{D_C}\,r_{0,C_A} + \sqrt{D_A}\,r_{0,C_C}\right)(j\omega)^{3/2} \\ +\sqrt{D_A D_C}\,r_{1,\Theta}(j\omega) \\ +\begin{pmatrix} \sqrt{D_C}\,r_{0,C_A}r_{1,\Theta} - \sqrt{D_A}\,r_{0,C_C}r_{1,\Theta} \\ -\sqrt{D_C}\,r_{0,\Theta}r_{1,C_A} + \sqrt{D_A}\,r_{0,\Theta}r_{1,C_C} \end{pmatrix}(j\omega)^{1/2} \end{bmatrix} \tag{13a}$$

$$= \frac{1}{2F}\left[ b_4(j\omega)^2 + b_3(j\omega)^{3/2} + b_2(j\omega) + b_1(j\omega)^{1/2} \right]$$

They are polynomials of the second order in $j\omega$. The faradaic impedance may then be calculated and simplified into:

$$\hat{Y}_f = -2F\frac{a_4(j\omega)^2 + a_2(j\omega)}{b_4(j\omega)^2 + b_3(j\omega)^{3/2} + b_2(j\omega) + b_1(j\omega)^{1/2}}$$

$$= -2F\left\{ \frac{a_4}{b_4} - \frac{a_4}{b_4}\left[ \frac{\frac{b_3}{b_4}(j\omega) + \left(\frac{b_2}{b_4} - \frac{a_2}{a_4}\right)(j\omega)^{1/2} + \frac{b_1}{b_4}}{(j\omega)^{3/2} + \frac{b_3}{b_4}(j\omega) + \frac{b_2}{b_4}(j\omega)^{1/2} + \frac{b_1}{b_4}} \right] \right\} \tag{14}$$

The first term is the inverse of the charge transfer resistance $R_{ct}^{-1} = -2Fa_4/b_4$. Further rearrangements of this equation are possible and the faradaic impedance may also be easily determined.

A general method of treating the electrochemical impedance of multistep mechanisms was presented by Harrington[2] and Harrington and Driessche.[3]

## III. HYDROGEN UPD

On several noble metals (Pt, Rh, Ru, Ir, Pd) hydrogen ion reduction takes place at the potentials positive to the equilibrium potential for hydrogen evolution. This is so-called hydrogen

underpotential deposition (H UPD) and indicates strong adsorptive interaction between atomic hydrogen and the metal. Similar UPD processes are observed for deposition of metals on metals[4]. Such a reaction may be written as:

$$H^+ + M + e \xrightarrow[\overleftarrow{k_{-1}}]{\vec{k}_1} MH_{ads}$$

$$\text{or} \tag{15}$$

$$H_2O + M + e \xrightarrow[\overleftarrow{k_{-1}}]{\vec{k}_1} MH_{ads} + OH^-$$
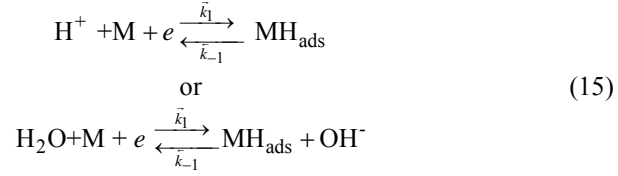
in acid and alkaline solutions, respectively. Assuming Langmuir adsorption isotherm for H, the rate of this reaction is given as:

$$i = \frac{dQ}{dt} = \sigma_1 \frac{d\Theta}{dt}$$
$$= F\left[ k_0 C_{H^+} \Gamma_s e^{-\beta f(E - E_1^0)} - k_0 \Gamma_H e^{(1-\beta)f(E - E_1^0)} \right] \tag{16}$$

where $Q$ is the charge corresponding to the adsorption of H, $\sigma_1$ is the charge necessary for attainment of monolayer coverage by adsorbed H, $k_0$ is the standard rate constant, $\Gamma_s$ is the surface concentration of free sites (in mol cm$^{-2}$), $\Gamma_H$ is the surface concentration of adsorbed H and $E_1^0$ is the standard potential of reaction (15). The fractional surface coverage by adsorbed H is $\Theta = \Gamma_H /(\Gamma_H + \Gamma_s) = \Gamma_H / \Gamma_\infty$, where $\Gamma_\infty = \Gamma_H + \Gamma_s$ is the total concentration of adsorption sites. The equilibrium potential for the H UPD reaction can be expressed as: $E_{eq} - E_1^0 = (RT/F)\ln[C_{H^+}^* (1-\Theta)/\Theta]$. Taking as a reference state the potential $E_p$ at which $\Theta = 0.5$ (corresponding to the peak potential on cyclic voltammograms, $E_p = E_1^0 + RT/F \ln C_{H^+}^*$) and introducing it into Eq. (16),

$$i = \sigma_1 \frac{d\Theta}{dt} = F v_1$$

$$= F \left[ k_0 C_{H^+}^{*\,1-\beta} \, \Gamma_\infty \Theta e^{-\beta f(E-E_p)} - k_0 C_{H^+}^{*\,1-\beta} \Gamma_\infty \, e^{(1-\beta)f(E-E_p)} \right] = \qquad (17)$$

$$= F \left[ \vec{k}_1 (1-\Theta) - \overleftarrow{k}_{-1} \Theta \right]$$

is obtained, where $\vec{k}_1$ and $\overleftarrow{k}_{-1}$ are potential dependent rate constants which also include concentration terms: $\vec{k}_1 = k_0 C_{H^+}^{*\,1-\beta} \Gamma_\infty \exp[-\beta f(E-E_p)]$ and $\overleftarrow{k}_{-1} = k_0 C_{H^+}^{*\,1-\beta} \Gamma_\infty \exp[(1-\beta) f(E-E_p)]$. Let us also introduce overpotential, defined here as $\eta = E - E_p$. The impedance of this process was developed by Harrington and Conway[5] and discussed by Lasia.[6,7] Equation (17) may be linearized as:

$$\frac{\Delta i}{F} = \Delta v_1 = \frac{\sigma_1}{F} \frac{d\Delta\Theta}{dt} = \left( \frac{\partial v_1}{\partial \eta} \right) \Delta\eta + \left( \frac{\partial v_1}{\partial \Theta} \right) \Delta\Theta \qquad (18)$$

or, introducing phasors (see Part I, Section 4.1, ref. 1),

$$\frac{\tilde{i}}{F} = j\omega \frac{\sigma_1}{F} \tilde{\Theta} = \left( \frac{\partial v_1}{\partial \eta} \right) \tilde{\eta} + \left( \frac{\partial v_1}{\partial \Theta} \right) \tilde{\Theta} \qquad (19)$$

results. These equations may be written in a matrix form:

$$\begin{bmatrix} -\dfrac{\partial v_1}{\partial \eta} \\[2ex] -\dfrac{\partial v_1}{\partial \eta} \end{bmatrix} = \begin{bmatrix} -\dfrac{1}{F} & \dfrac{\partial v_1}{\partial \Theta} \\[2ex] 0 & \dfrac{\partial v_1}{\partial \Theta} - j\omega \dfrac{\sigma_1}{F} \end{bmatrix} \begin{bmatrix} \dfrac{\tilde{i}}{\tilde{\eta}} \\[2ex] \dfrac{\tilde{\Theta}}{\tilde{\eta}} \end{bmatrix} \qquad (20)$$

and the faradaic admittance $\hat{Y}_f = -\tilde{i}/\tilde{\eta}$ is then

$$\hat{Y}_f = -F\left(\frac{\partial v_1}{\partial \eta}\right) - \frac{F\left(\frac{\partial v_1}{\partial \eta}\right)\frac{F}{\sigma_1}\left(\frac{\partial v_1}{\partial \Theta}\right)}{j\omega - \frac{F}{\sigma_1}\left(\frac{\partial v_1}{\partial \Theta}\right)} = A - \frac{AC}{j\omega + C} \tag{21}$$

where $\quad A = 1/R_{ct} = -F\left(\partial v_1/\partial \eta\right)\quad$ and $\quad C = -\left(F/\sigma_1\right)\left(\partial v_1/\partial \Theta\right)$. The faradaic impedance follows as:

$$\hat{Z}_f = \frac{1}{\hat{Y}_f} = \frac{1}{A} + \frac{1}{j\omega(A/C)} = R_{ct} + \frac{1}{j\omega C_p} \tag{22}$$

This equation corresponds to a connection of the charge transfer resistance, $R_{ct}$, and the capacitance, $C_p$, in series. It is an analog of Eq. (143), Part I, the corresponding complex plane plot represents a semicircle followed by a capacitive line was shown in Figure 23 (Part I). The total impedance consists of the solution resistance, $R_s$, in series with the parallel connection of the double-layer capacitance, $C_{dl}$, giving the faradaic impedance:

$$\hat{Z} = R_s + \frac{1}{j\omega C_{dl} + \dfrac{1}{\hat{Z}_f}} \tag{23}$$

On solid electrodes, very often $C_{dl}$ must be substituted by a constant-phase element (see Part 1, Section V.2, ref.1)

$$\hat{Z} = R_s + \frac{1}{(j\omega)^{\phi} T + \dfrac{1}{\hat{Z}_f}} \tag{24}$$

Assuming transfer coefficients as equal to 0.5, the equivalent circuit parameters may be described as:

$$R_{ct} = \frac{1}{fF}\left(\frac{1}{\vec{k}_1} + \frac{1}{\vec{k}_{-1}}\right) = \frac{2RT}{F^2 k_0}\cosh(0.5f\eta) \tag{25}$$

It should be noticed that the pseudocapacitance $C_p$ is independent of the rate constants; hence the kinetic information may be obtained only from the charge-transfer resistance. Assuming that $\sigma_1 = 210\ \mu C\ cm^{-2}$ [8], the following values of the equivalent electrical circuit elements are obtained at $\eta = 0$ [6,7]:

$$R_{ct} = \frac{2RT}{F^2 k_0} = \frac{5.33\times10^{-7}}{k_0}\ \Omega\ cm^2$$

$$C_p = \frac{F\sigma_1}{4RT} = 2.04\ mF\ cm^{-2} \tag{26}$$
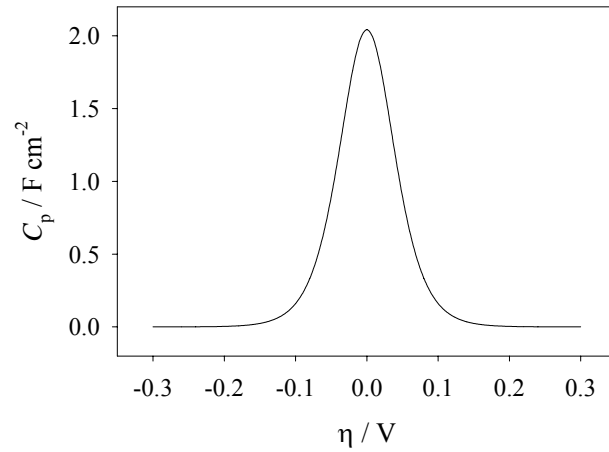


**Figure 1.** Dependence of the adsorption pseudocapacitance of the hydrogen UPD on overpotential assuming Langmuir isotherm.

The dependences of $C_p$ and log $R_{ct}$ on overpotential are shown in Figure 1 and 2, respectively. In Figure 1 a maximum of $C_p$ and in Figure 2 a minimum of $R_{ct}$ arises at $E_p$, that is for $\eta = 0$. In the case of symmetry coefficients different from 0.5, the minimum of $R_{ct}$ is slightly shifted (see Part I, Section III.2, ref. 1).

However, more complex behavior is observed experimentally. On polycrystalline platinum two voltammetric peaks are observed; this indicates a distribution of adsorption energies and/or a more complex adsorption isotherm. Plots of the experimental impedance on polycrystalline Pt show a capacitive behavior[6,7] but the analysis allowed only determination of the pseudocapacitance, which was identical with that determined using cyclic voltammetry. The maximal capacitance was ~1.2 mF cm$^{-2}$, which is lower than the maximal value for Langmurian behavior indicating that the experimental isotherm is more complex.
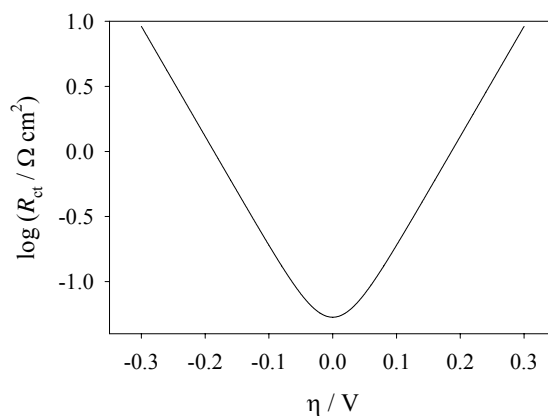


**Figure 2.** Dependence of the logarithm of the charge transfer resistance on overpotential for $k_0 = 10^{-5}$ mol cm$^{-2}$ s$^{-1}$, assuming Langmuir isotherm.
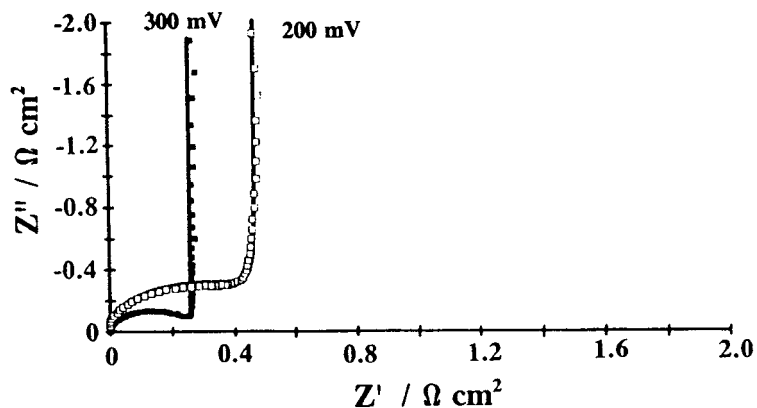
**Figure 3.** Complex-plane plots for Pt(100) in 0.5 M $H_2SO_4$ at two potentials. The solid lines correspond to fitting of the data using the equivalent circuit described by Eqs. (22) and (24).[9]

Morin et al.[9] studied the UPD of H on Pt single-crystal electrodes. The obtained complex plane plots resembling those predicted theoretically; an example obtained on Pt(100) in 0.5 M $H_2SO_4$ is shown in Figure 3 (note that deformation is connected with different scales being used for the two axes).

Analysis according to Eq. (22) for an equivalent circuit containing solution resistance, $R_s$, and double-layer capacitance, $C_{dl}$, allowed all of the parameters to be determined. An example of the dependence of $C_p$, $C_{dl}$, and $R_{ct}$ on electrode potential for Pt(100) is shown in Figure 4. It is surprising that $R_{ct}$ is practically potential independent over a wide potential range and $C_{dl}$ and $C_p$ seem to be correlated. It was also found that at more positive potentials on Pt(311) there is an influence of anionic ($HSO_4^-$) adsorption. In the equivalent circuit, an additional element containing connection $R_{p2}$-$C_{p2}$ in series should be added in parallel with the faradaic impedance, Eq. (22). Further studies of the H UPD adsorption isotherm should explain this complex adsorption

behavior. It should be added that these measurements are difficult because of the high H UPD rate. Harrington[10] has applied ac voltammetry to the study of hydrogen UPD and has determined the fastest sweep rate which can be used without affecting the slow ac response.

It should be added that similar mathematical treatment might be carried out for the UPD of metals.

## IV. THE HYDROGEN EVOLUTION REACTION

### 1. The HER in the absence of mass-transfer effects

The hydrogen evolution reaction is one of the most often-studied electrocatalytic reactions. It is well accepted that the reaction mechanism usually proceeds through three steps[5-7, 11, 12]: (i) electrochemical adsorption or the Volmer reaction, (15), and two possible desorption steps: (ii) electrochemical desorption, the Heyrovsky reaction, (28), and (iii) chemical desorption, the Tafel reaction, (29). They may be written for the reactions in acidic or alkaline solutions:

$$H^+ + M + e \xrightleftharpoons[\vec{k}_{-1}]{\vec{k}_1} MH_{ads}$$

$$\text{or} \tag{27}$$

$$H_2O + M + e \xrightleftharpoons[\vec{k}_{-1}]{\vec{k}_1} MH_{ads} + OH^-$$

$$MH + H^+ + e \xrightleftharpoons[\vec{k}_{-2}]{\vec{k}_2} M + H_2$$

$$\text{or} \tag{28}$$

$$MH + H_2O + e \xrightleftharpoons[\vec{k}_{-2}]{\vec{k}_2} M + OH^- + H_2$$

**a)**



**b)**



**c)**



$E \ / \ V$ (vs RHE)
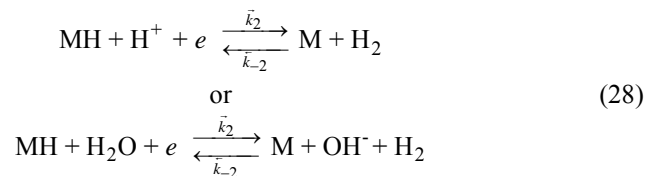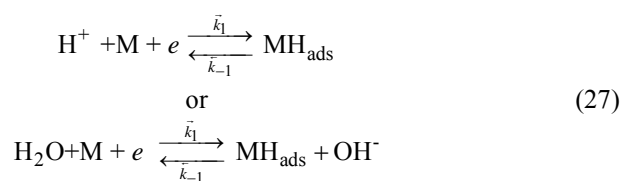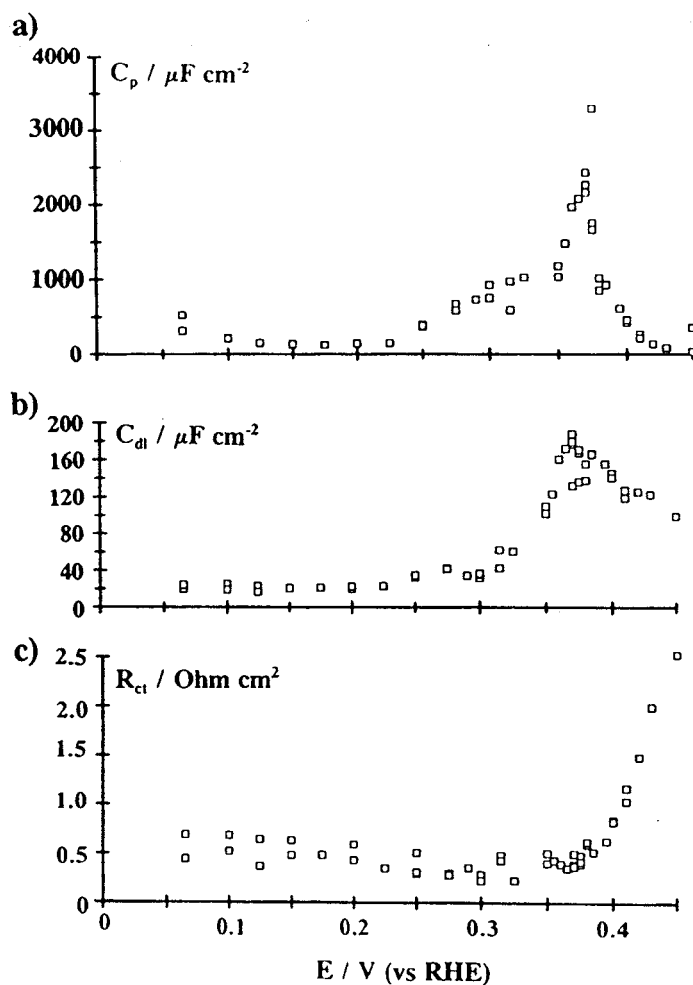
**Figure 4.** (a) Pseudocapacitance $C_p$, (b) double layer capacitance $C_{dl}$ and (c) charge transfer resistance $R_{ct}$ as a function of the applied potential (vs. RHE) for the H UPD on a Pt(100) electrode in 0.5 M $H_2SO_4$.[9]

$$2 \ MH \ \xrightleftharpoons[k_{-3}]{k_3} \ 2 \ M + H_2 \tag{29}$$
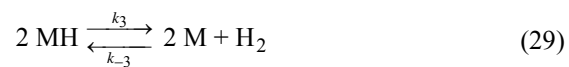
These reaction steps involve H adsorbed on the electrode surface (case of one adsorbed species, see Section IV-1, Part I, ref. 1). Below, kinetic equations will be presented for hydrogen evolution in alkaline solutions but similar equations may be easily written for the reactions in acidic media. Assuming a Langmuir adsorption isotherm for H on the electrode surface, the rates, $v_i$ (in mol cm$^{-2}$ s$^{-1}$), of these reactions are:

$$v_1 = k_{1,0}^0 a_{H_2O} \Gamma_s \, e^{-\beta_1 f\left(E-E_1^0\right)} - k_{1,0}^0 a_{OH^-} \Gamma_H \, e^{(1-\beta_1)f\left(E-E_1^0\right)} \tag{30}$$

$$v_2 = k_{2,0}^0 a_{H_2O} \Gamma_H \, e^{-\beta_2 f\left(E-E_2^0\right)} - k_{2,0}^0 a_{H_2} a_{OH^-} \Gamma_s \, e^{(1-\beta_2)f\left(E-E_2^0\right)} \tag{31}$$

$$v_3 = k_{3,0}^0 \Gamma_H^2 - k_{3,0}^0 \Gamma_s^2 a_{H_2} \tag{32}$$

where $k_{i,0}^0$ are the standard reaction rate constants, $E_i^0$ the standard electrode potentials, $\Gamma_H$ and $\Gamma_s$ the surface concentrations of adsorbed H and that of free sites (in mol cm$^{-2}$), and $\beta_i$ symmetry coefficients. Introducing the surface coverages, $\Theta = \Gamma_H / \Gamma_{H,max}$ and $1 - \Theta = \Gamma_s / \Gamma_{H,max}$, and the overpotential $\eta = E - E_{eq}$, the following equations are obtained:

$$
\begin{aligned}
v_1 = {}& k_1^0 a_{H_2O} \left(1-\Theta\right) \left[ \left(\frac{\Theta_0}{1-\Theta_0}\right) \frac{a_{OH^-,0}}{a_{H_2O,0}} \right]^{\beta_1} e^{-\beta_1 f\eta} \\
& - k_1^0 a_{OH^-} \Theta \left( \frac{1-\Theta_0}{\Theta_0} \frac{a_{H_2O,0}}{a_{OH^-,0}} \right)^{1-\beta_1} e^{(1-\beta_1)f\eta}
\end{aligned}
\tag{33}
$$

$$v_2 = k_2^0 a_{H_2O} \Theta \left( \frac{1-\Theta_0}{\Theta_0} \frac{a_{H_2,0} a_{OH^-,0}}{a_{H_2O,0}} \right)^{\beta_2} e^{-\beta_2 f \eta}$$

$$- k_2^0 a_{H_2} a_{OH^-} (1-\Theta) \left( \frac{\Theta_0}{1-\Theta_0} \frac{a_{H_2O,0}}{a_{H_2,0} a_{OH^-,0}} \right)^{1-\beta_2} e^{(1-\beta_2) f \eta} \tag{34}$$

$$v_3 = k_3^0 \Theta^2 - k_3^0 (1-\Theta)^2 a_{H_2} \tag{35}$$

where: $k_1^0 = k_{1,0}^0 \Gamma_{H,max}$, $k_2^0 = k_{2,0}^0 \Gamma_{H,max}$, $k_3^0 = k_{3,0}^0 \Gamma_{H,max}^2$, and index "0" indicates parameters measured at $\eta = 0$. These equations may subsequently be rearranged into:

$$v_1 = v_{1,0} \left( \frac{a_{H_2O}}{a_{H_2O,0}} \right) \left( \frac{1-\Theta}{1-\Theta_0} \right) e^{-\beta_1 f \eta} - v_{1,0} \left( \frac{a_{OH^-}}{a_{OH^-,0}} \right) \frac{\Theta}{\Theta_0} e^{(1-\beta_1) f \eta} \tag{36}$$

$$v_2 = v_{2,0} \left( \frac{a_{H_2O}}{a_{H_2O,0}} \right) \frac{\Theta}{\Theta_0} e^{-\beta_2 f \eta}$$

$$- v_{2,0} \left( \frac{a_{OH^-}}{a_{OH^-,0}} \right) \left( \frac{a_{H_2}}{a_{H_2,0}} \right) \left( \frac{1-\Theta}{1-\Theta_0} \right) e^{(1-\beta_2) f \eta} \tag{37}$$

$$v_3 = v_{3,0} \left[ \frac{\Theta^2}{\Theta_0^2} - \frac{(1-\Theta)^2}{(1-\Theta_0)^2} \frac{a_{H_2}}{a_{H_2,0}} \right] \tag{38}$$

where $v_{i,0}$ is the reaction rate in each direction at the equilibrium potential. When concentration polarization may be neglected, these equations simplify to:

$$v_1 = k_1 (1-\Theta) e^{-\beta_1 f \eta} - k_{-1} \Theta e^{(1-\beta_1) f \eta} = \vec{k}_1 (1-\Theta) - \overleftarrow{k}_{-1} \Theta \tag{39}$$

$$v_2 = k_2 \Theta e^{-\beta_2 f \eta} - k_{-2}(1-\Theta) e^{(1-\beta_2)f\eta} = \vec{k}_2 \Theta - \bar{k}_{-2}(1-\Theta) \tag{40}$$

$$v_3 = k_3 \Theta^2 - k_{-3}(1-\Theta)^2 \tag{41}$$

From the condition $\eta = 0$, it also follows that:

$$\frac{k_1 k_2}{k_{-1} k_{-2}} = \frac{k_1^2 k_3}{k_{-1}^2 k_{-3}} = 1 \tag{42}$$

In the steady-state $v_1 - v_2 - 2v_3 = 0$ and the dc surface coverage is given by

$$\Theta = \frac{\vec{k}_1 + \bar{k}_{-1}}{\vec{k}_1 + \bar{k}_{-1} + \vec{k}_2 + \bar{k}_{-2}} \tag{43}$$

In general, to describe the hydrogen evolution kinetics, it is necessary to determine four (out of six) rate constants and two transfer coefficients. Such a procedure is quite difficult and the results of dc and ac experiments must be used to determine these parameters. In order to evaluate the reaction impedance, a linearization method is used, as described in Section IV-1, Part 1, ref.1:

$$\Delta i = \left(\frac{\partial i}{\partial \eta}\right)_\Theta \Delta \eta + \left(\frac{\partial i}{\partial \Theta}\right)_\eta \Delta \Theta = F\left[\left(\frac{\partial r_0}{\partial \eta}\right)_\Theta \Delta \eta + \left(\frac{\partial r_0}{\partial \Theta}\right)_\eta \Delta \Theta\right] \tag{44}$$

$$\frac{\sigma_1}{F}\frac{d\Delta\Theta}{dt} = \Delta r_1 = \left(\frac{\partial r_1}{\partial \eta}\right)_\Theta \Delta \eta + \left(\frac{\partial r_1}{\partial \Theta}\right)_\eta \Delta \Theta \tag{45}$$

where $r_0 = v_1 + v_2$ and $r_1 = v_1 - v_2 - v_3$. Introducing phasors for $\Theta$, $\eta$, $i$ and $r_i$ results in

$$\frac{\tilde{i}}{F} = \tilde{r}_0 = \left(\frac{\partial r_0}{\partial \eta}\right)_\Theta \tilde{\eta} + \left(\frac{\partial r_0}{\partial \Theta}\right)_\eta \tilde{\Theta} \tag{46}$$

$$\frac{\sigma_1}{F} j\omega \tilde{\Theta} = \left(\frac{\partial r_1}{\partial \eta}\right)_\Theta \tilde{\eta} + \left(\frac{\partial r_1}{\partial \Theta}\right)_\eta \tilde{\Theta} \tag{47}$$

These equations may be represented in matrix form as

$$\begin{bmatrix} -\dfrac{\partial r_0}{\partial \eta} \\[2ex] -\dfrac{\partial r_1}{\partial \eta} \end{bmatrix} = \begin{bmatrix} \dfrac{-1}{F} & \dfrac{\partial r_0}{\partial \Theta} \\[2ex] 0 & \dfrac{\partial r_1}{\partial \Theta} - j\omega\dfrac{\sigma_1}{F} \end{bmatrix} \begin{bmatrix} \dfrac{\tilde{i}}{\tilde{\eta}} \\[2ex] \dfrac{\tilde{\Theta}}{\tilde{\eta}} \end{bmatrix} \tag{48}$$

giving the faradaic impedance as:

$$\hat{Y}_f = -\frac{\tilde{i}}{\tilde{\eta}} = -F\left(\frac{\partial r_0}{\partial \eta}\right)_\Theta - \frac{\dfrac{F^2}{\sigma_1}\left(\dfrac{\partial r_0}{\partial \Theta}\right)_\eta\left(\dfrac{\partial r_1}{\partial \eta}\right)_\Theta}{j\omega - \dfrac{F}{\sigma_1}\left(\dfrac{\partial r_1}{\partial \Theta}\right)_\eta} = A + \frac{B}{j\omega + C} \tag{49}$$

where

$$A = -F\left(\frac{\partial r_0}{\partial \eta}\right)_\Theta, \quad B = -\frac{F^2}{\sigma_1}\left(\frac{\partial r_0}{\partial \Theta}\right)_\eta\left(\frac{\partial r_1}{\partial \eta}\right)_\Theta,$$

$$\text{and } C = -\frac{F}{\sigma_1}\left(\frac{\partial r_1}{\partial \Theta}\right)_\eta \tag{50}$$

The faradaic admittance, Eq. (49), may be written as a corresponding impedance:

$$\hat{Z}_f = R_{ct} + \frac{1}{j\omega C_p + \dfrac{1}{R_p}} \qquad (51)$$

see also Part I, Chapter IV.2, ref.1, where:

$$R_{ct} = \frac{1}{A}, \quad C_p = -\frac{A^2}{B}, \quad R_p = -\frac{1}{\dfrac{A^2 C}{B} + A} \qquad (52)$$

Equation (49) is identical with Eq. (135), Part I, the only difference is the definition of the parameter $r_1$. As was shown in Part I, this process may produce two semi-circles on the complex plane plots. Such plots have been observed for the HER on Pt,[13,14] Ni-Fe,[15] Ru,[16,17] Rh,[18] electrocodeposited Raney Ni.[19,20] However, one semicircle is usually observed in the complex plane plots of Ni[21] and Ni-based rough and porous electrodes such as Ni-Zn alloy,[22] Ni-B,[23,24] Ni-P,[25] Ni-Zn-P,[26] etc. For some electrode materials (Ni-Zn[27,28] and Ni-Al[29,28] pressed powders), surface porosity causes appearance of two semi-circles in the complex plane plots, with the first one being connected with surface porosity, Section V-4 (iii), Part I. In other cases, de Levie's porous or fractal models have been used.[25, 30-33]

## 2. In the presence of hydrogen mass-transfer

Recently, the influence of the mass transfer of evolved hydrogen was evidenced for the HER on single crystal Pt surfaces in $H_2SO_4$.[34, 35] Activity of Pt(hkl) depends on the crystallographic orientations[36] and effects of hydrogen diffusion from the electrode are observed on the rotating disk electrode. In order to deal with this problem, Eqs. (40) and (41) should be rearranged, using Eqs. (37) and (38). Neglecting the mass-transfer limitations of protons towards the electrode one obtains (concentrated acid solution):

$$v_2 = \vec{k}_2 \Theta - \bar{k}_{-2}(1-\Theta)\left(C_0/C^*\right) \tag{53}$$

and

$$v_3 = k_3 \Theta^2 - k_{-3}(1-\Theta)^2 \left(C_0/C^*\right) \tag{54}$$

where $C_0$ and $C^*$ are the surface and bulk hydrogen ($H_2$) concentrations, respectively. Current, surface coverage changes and the diffusional flux of hydrogen may be written as:

$$i = F\left(v_1 + v_2\right) = Fr_0 \tag{55}$$

$$\frac{\sigma_1}{F}\frac{d\Theta}{dt} = v_1 - v_2 - 2v_3 = r_1 \tag{56}$$

$$J_{H2} = -D_{H_2}\frac{dC_0}{dx} = v_2 + v_3 = r_2 \tag{57}$$

where $J_{H_2}$ is the flux of dissolved hydrogen and $D_{H_2}$ its diffusion coefficient. For the rotating disk electrode, the flux is: $J_{H_2} = D_{H_2}(C_0 - C^*)/\delta$ where the diffusion layer thickness is given by: $\delta = 1.612 D^{1/3} v^{1/6} \Omega^{-1/2}$, with $v$ being the kinematic viscosity and $\Omega$ the rotation frequency. In order to determine the faradaic impedance Eqs. (55)-(57) must be expressed as phasors. The diffusional flux of hydrogen, for the rotating-disk electrode (finite length diffusion, transmissive conditions) is expressed as:

$$\tilde{J}_{H_2} = \tilde{C}_0 \sqrt{j\omega D_{H_2}}\, \coth\left(\sqrt{\frac{j\omega}{D_{H_2}}}\delta\right) = J'\tilde{C}_0 \tag{58}$$

$$\tilde{i} = F\left[\left(\frac{\partial r_0}{\partial \eta}\right)\tilde{\eta} + \left(\frac{\partial r_0}{\partial \Theta}\right)\tilde{\Theta}\right] \tag{59}$$

$$j\omega \frac{\sigma_1}{F} \tilde{\Theta} = \left(\frac{\partial r_1}{\partial \eta}\right)\tilde{\eta} + \left(\frac{\partial r_1}{\partial \Theta}\right)\tilde{\Theta} + \left(\frac{\partial r_1}{\partial C_0}\right)\tilde{C}_0 \tag{60}$$

$$\tilde{C}_0 \sqrt{j\omega D_{H_2}} \coth\left(\sqrt{\frac{j\omega}{D_{H_2}}}\delta\right) = \left(\frac{\partial r_2}{\partial \Theta}\right)\tilde{\Theta} + \left(\frac{\partial r_2}{\partial C_0}\right)\tilde{C}_0 \tag{61}$$

They may be written in a matrix form:

$$\begin{bmatrix} -\dfrac{\partial r_0}{\partial \eta} \\[2mm] -\dfrac{\partial r_1}{\partial \eta} \\[2mm] 0 \end{bmatrix} = \begin{bmatrix} -\dfrac{1}{F} & \dfrac{\partial r_0}{\partial \Theta} & 0 \\[2mm] 0 & \dfrac{\partial r_1}{\partial \Theta} - j\omega\dfrac{\sigma_1}{F} & \dfrac{\partial r_1}{\partial C_0} \\[2mm] 0 & \dfrac{\partial r_2}{\partial \Theta} & \dfrac{\partial r_2}{\partial C_0} - J' \end{bmatrix} \begin{bmatrix} \dfrac{\tilde{i}}{\tilde{\eta}} \\[2mm] \dfrac{\tilde{\Theta}}{\tilde{\eta}} \\[2mm] \dfrac{\tilde{C}_0}{\tilde{\eta}} \end{bmatrix} \tag{62}$$

The faradaic admittance is then:

$$\hat{Y}_f = A + \cfrac{B}{j\omega + C + \cfrac{D}{E - J'}} \tag{63}$$

where $A$, $B$, and $C$ were defined in Eq. (50) and the parameters $D$ and $E$ are:

$$D = \frac{F}{\sigma_1}\left(\frac{\partial r_1}{\partial C_0}\right)\left(\frac{\partial r_2}{\partial \Theta}\right) \quad \text{and} \quad E = \left(\frac{\partial r_2}{\partial C_0}\right) \tag{64}$$

Equation (63) differs from Eq. (49) by the presence of the additional term in the denominator. It may be further simplified by assuming the Volmer-Tafel mechanism. It can be rearranged into a faradaic impedance:

$$\hat{Z}_f = R_{ct} + \cfrac{1}{j\omega C_p + R_p^{-1} + \cfrac{1}{R_{des} + \hat{Z}_W}} \tag{65}$$

where

$$R_{des} = -\frac{BE}{A^2 D}, \quad \hat{Z}_W = \frac{B}{A^2 D}\sqrt{j\omega D_{H_2}}\coth\left(\sqrt{\frac{j\omega}{D_{H_2}}}\delta\right) \tag{66}$$

Equation (65) differs from Eq. (49) by the presence of a new parallel branch in the equivalent circuit, containing connection of a desorption resistance $R_{des}$ and mass transfer impedance $\hat{Z}_W$ in series (note typing errors in the original publications, cited as refs. 34 and 35).

Determination of the kinetic parameters of the hydrogen evolution reaction is usually carried out by simultaneous approximation of the dc current and the parameters obtained from the impedance technique (*A, B, C*) by adjusting the kinetic parameters (rate constants); however, several authors used approximation of the EIS data only.[11,12,16-25, 27-32, 34-40]


# V. HYDROGEN ABSORPTION INTO METAL ELECTRODES

## 1. Hydrogen adsorption, absorption and evolution: Linear diffusion

We now consider the hydrogen evolution reaction at negative overpotentials, Eqs. (15), (28) and (29), accompanied by the process of H absorption into the cathode material:

$$\text{MH}_{\text{ads}} \xrightleftharpoons[k_{-4}]{k_4} \text{MH}_{\text{abs}} \tag{67}$$

followed by diffusion of hydrogen into the bulk metal.[41] This process is observed on hydrogen-absorbing metals (Pd) and alloys (e.g. $\text{LaNi}_5$). Let it be supposed that a metallic layer of the thickness $l$ is deposited on a non-absorbing support, from which hydrogen cannot escape. The same reasoning may be applied to H deposition on a metallic foil immersed in the solution; in this case the layer thickness $l$ is half the thickness of the foil. The rate of such a reaction is given by:

$$v_4 = k_4 \Theta (1 - X_0) - k_{-4}(1 - \Theta) X_0 \tag{68}$$

where $X = C_H / C_{H,max}$ is the dimensionless H concentration inside the metal, i.e. the ratio of the H concentration to the maximal possible H concentration, and index 0 indicates the concentration at the electrode surface, $x = 0$, inside the absorbing metal. The dimensionless H concentration changes between 0 and 1. Under steady-state conditions, defined in this way, the rate of reaction (67) is null, which leads to:

$$X_0 = \frac{k_4 \Theta}{k_4 \Theta + k_{-4}(1 - \Theta)} \tag{69}$$

In order to solve this problem the diffusion of H into the metal must be taken into account through the Fick's second equation:[42-48]

$$\frac{\partial X}{\partial t} = D_H \frac{\partial^2 X}{\partial x^2} \tag{70}$$

while the H flux at the surface is given by

$$J_H = -D_H \frac{\sigma_x}{F} \left( \frac{\partial X}{\partial x} \right)_{x=0} = v_4 \tag{71}$$

where $\sigma_x = FC_{H,max}$ is the charge corresponding to the saturation of metal with hydrogen. Eq. (71) may be solved for the oscillating concentration: $\Delta X = \tilde{X}\exp(j\omega t)$, where $\tilde{X}$ is the concentration phasor, see Part 1 , Eq. (41). The equation obtained is analogous to Eq. (47), Part 1; thus

$$j\omega\tilde{X} = D_H \frac{d^2\tilde{X}}{dx^2} \tag{72}$$

with the boundary conditions:

$$
\begin{aligned}
x = 0 && -D_H \frac{\sigma_x}{F}\frac{d\tilde{X}}{dx} = \tilde{J}_H \\
x = l && \frac{d\tilde{X}}{dx} = 0
\end{aligned}
\tag{73}
$$

where $J$ is the flux of H. The solution of Eq. (72) is:

$$\tilde{X} = A\,e^{-sx} + B\,e^{sx} \tag{74}$$

where $s = \sqrt{j\omega/D_H}$ . Taking into account the boundary conditions, one obtains:

$$\tilde{X} = \frac{F}{\sigma_x}\frac{\tilde{J}_H}{\sqrt{j\omega D_H}}\frac{e^{s(l-x)}+e^{-s(l-x)}}{e^{sl}-e^{-sl}} \tag{75}$$

and the surface concentration is

$$\tilde{X}_0 = \frac{F}{\sigma_x}\frac{\tilde{J}_H}{\sqrt{j\omega D_H}}\coth\left(\sqrt{\frac{j\omega}{D_H}}\,l\right) \tag{76}$$

The oscillating flux is represented by:

$$\tilde{J}_H = \frac{\sigma_x}{F}\tilde{X}_0\sqrt{j\omega D_H}\ \tanh\left(\sqrt{\frac{j\omega}{D_H}}l\right) = \left(\frac{\partial v_4}{\partial\Theta}\right)\tilde{\Theta} + \left(\frac{\partial v_4}{\partial X_0}\right)\tilde{X}_0 \qquad (77)$$

or

$$\tilde{J}_H = \tilde{X}_0 J_H' \quad \text{where} \quad J_H' = \frac{\sigma_x}{F}\sqrt{j\omega D_H}\ \tanh\left(\sqrt{\frac{j\omega}{D_H}}l\right) \qquad (78)$$

Now, knowing the diffusional flux, it is possible to calculate the total impedance. As in Section IV, the current is given as:

$$\frac{\Delta i}{F} = \Delta r_0 = \Delta v_1 + \Delta v_2 \qquad (79)$$

And $\tilde{r}_0$ by

$$\tilde{r}_0 = \frac{\tilde{i}}{F} = \left(\frac{\partial r_0}{\partial\eta}\right)\tilde{\eta} + \left(\frac{\partial r_0}{\partial\Theta}\right)\tilde{\Theta} \qquad (80)$$

Similar reasoning should be applied for d$\Delta\Theta$/dt, i.e.,

$$\begin{aligned}
\frac{\sigma_1}{F}\frac{d\tilde{\Theta}}{dt} &= \frac{\sigma_1}{F}j\omega\tilde{\Theta} = \tilde{v}_1 - \tilde{v}_2 - 2\tilde{v}_3 - \tilde{v}_4 = \tilde{r}_1 - \tilde{v}_4 \\
&= \left(\frac{\partial r_1}{\partial\Theta}\right)\tilde{\Theta} + \left(\frac{\partial r_1}{\partial\eta}\right)\tilde{\eta} - \left(\frac{\partial v_4}{\partial\Theta}\right)\tilde{\Theta} - \left(\frac{\partial v_4}{\partial X_0}\right)\tilde{X}_0
\end{aligned} \qquad (81)$$

where $r_1 = v_1 - v_2 - 2v_3$. Equations (77), (80) and (81) can be transformed into matrix form as:

$$
\begin{bmatrix} -\dfrac{\partial r_0}{\partial \eta} \\[2ex] -\dfrac{\partial r_1}{\partial \eta} \\[2ex] 0 \end{bmatrix} = \begin{bmatrix} -\dfrac{1}{F} & \dfrac{\partial r_0}{\partial \Theta} & 0 \\[2ex] 0 & \dfrac{\partial r_1}{\partial \Theta} - \dfrac{\partial v_4}{\partial \Theta} - j\omega\dfrac{\sigma_1}{F} & -\dfrac{\partial v_4}{\partial X_0} \\[2ex] 0 & \dfrac{\partial v_4}{\partial \Theta} & \dfrac{\partial v_4}{\partial X_0} - J_{\mathrm{H}}' \end{bmatrix} \begin{bmatrix} \dfrac{\tilde{i}}{\tilde{\eta}} \\[2ex] \dfrac{\tilde{\Theta}}{\tilde{\eta}} \\[2ex] \dfrac{\tilde{X}_0}{\tilde{\eta}} \end{bmatrix} \tag{82}
$$

The system can be simplified because of $\left(\partial r_1 / \partial X_0\right) = 0$. The solution, using Crammer's rule for $\tilde{i}_f / \tilde{\eta}$, is given as $\tilde{i}_f / \tilde{\eta} = T_1/B$ where:

$$
T_1 = \begin{vmatrix} -\dfrac{\partial r_0}{\partial \eta} & \dfrac{\partial r_0}{\partial \Theta} & 0 \\[2ex] -\dfrac{\partial r_1}{\partial \eta} & \dfrac{\partial r_1}{\partial \Theta} - \dfrac{\partial v_4}{\partial \Theta} - j\omega\dfrac{\sigma_1}{F} & -\dfrac{\partial v_4}{\partial X_0} \\[2ex] 0 & \dfrac{\partial v_4}{\partial \Theta} & \dfrac{\partial v_4}{\partial X_0} - J_{\mathrm{H}}' \end{vmatrix} \tag{83}
$$

$$
B = \begin{vmatrix} -\dfrac{1}{F} & \dfrac{\partial r_0}{\partial \Theta} & 0 \\[2ex] 0 & \dfrac{\partial r_1}{\partial \Theta} - \dfrac{\partial v_4}{\partial \Theta} - j\omega\dfrac{\sigma_1}{F} & -\dfrac{\partial v_4}{\partial X_0} \\[2ex] 0 & \dfrac{\partial v_4}{\partial \Theta} & \dfrac{\partial v_4}{\partial X_0} - J_{\mathrm{H}}' \end{vmatrix} \tag{84}
$$

and the admittance is:

$$\hat{Y}_f = -\frac{\tilde{i}}{\tilde{\eta}} = -F\left(\frac{\partial r_0}{\partial \eta}\right) - \frac{\dfrac{F^2}{\sigma_1}\left(\dfrac{\partial r_0}{\partial \Theta}\right)\left(\dfrac{\partial r_1}{\partial \eta}\right)}{j\omega - \dfrac{F}{\sigma_1}\left(\dfrac{\partial r_1}{\partial \Theta}\right) + \dfrac{\dfrac{F}{\sigma_1}\left(\dfrac{\partial v_4}{\partial \Theta}\right)}{1 - \dfrac{\left(\dfrac{\partial v_4}{\partial X_0}\right)}{J_H^{'}}}}$$

(85)

or

$$\tilde{Y}_f = A + \frac{B}{j\omega + C + \dfrac{D}{1 + \dfrac{E}{\sqrt{j\omega D_H}\,\tanh\left(\sqrt{\dfrac{j\omega}{D_H}}\,l\right)}}}$$

(86)

where the parameters $A$, $B$ and $C$ were defined earlier and $D$ and $E$ are defined as: $D = (F/\sigma_1)(\partial v_4/\partial \Theta)$ and $E = -(F/\sigma_x)(\partial v_4/\partial X_0)$. This equation should be compared with Eq. (49) for the HER; the difference is the additional term in the denominator, related to the hydrogen adsorption/absorption process. In order to relate to an electric equivalent circuit, Eq. (86) should be rearranged into impedance form:

$$\hat{Z}_f = 1/\hat{Y}_f$$

$$= \frac{1}{A} - \cfrac{1}{j\omega\left(\dfrac{A^2}{B}\right) + \left(\dfrac{A^2 C}{B} + A\right) + \cfrac{1}{\left(\dfrac{B}{A^2 D}\right) + \left(\dfrac{BE}{A^2 D}\right)\dfrac{\coth\left(\sqrt{\dfrac{j\omega}{D_\mathrm{H}}}l\right)}{\sqrt{j\omega D_\mathrm{H}}}}} =$$

$$= R_{ct} + \cfrac{1}{j\omega C_p + \dfrac{1}{R_p} + \cfrac{1}{R_{ab} + \cfrac{\sigma'\coth\left(\sqrt{\dfrac{j\omega}{D_\mathrm{H}}}l\right)}{\sqrt{j\omega D_\mathrm{H}}}}} = \tag{87}$$

$$= R_{ct} + \cfrac{1}{j\omega C_p + \dfrac{1}{R_p} + \dfrac{1}{R_{ab} + \hat{Z}_W}}$$

where $R_{ct}$, $R_p$ and $C_p$ were defined in Eq. (52) and other terms are defined below (see also Part I, Section IV.2, ref. 1):

$$R_{ab} = -\frac{B}{A^2 D} = \frac{1}{C_p}\frac{1}{D}; \qquad \sigma' = -\frac{BE}{A^2 D} = \frac{1}{C_p}\frac{E}{D};$$

$$\hat{Z}_W = \frac{\sigma'}{\sqrt{j\omega D_\mathrm{H}}}\coth\left(\sqrt{\frac{j\omega}{D_\mathrm{H}}}l\right) \tag{88}$$

$\hat{Z}_W$ corresponds to the mass-transfer impedance for finite-length diffusion and a reflecting interface, see Part 1, Eqs. (98)-(99). The units of $\sigma'$ are $\Omega$ cm$^3$ s$^{-1}$ and the other elements are expressed in their usual units ($\Omega$ cm$^2$, F cm$^{-2}$). For large $l$, $\coth(x) \to 1$ and $\hat{Z}_W$ becomes the impedance for semiinfinite diffusion; see Part 1, Eqs. (61) and (63). Equation (87) corresponds to the circuit shown in Figure 5. The only difference between the HER case and the hydrogen evolution-absorption mechanism is the presence of the additional parallel branch $R_{ab} + \hat{Z}_W$.
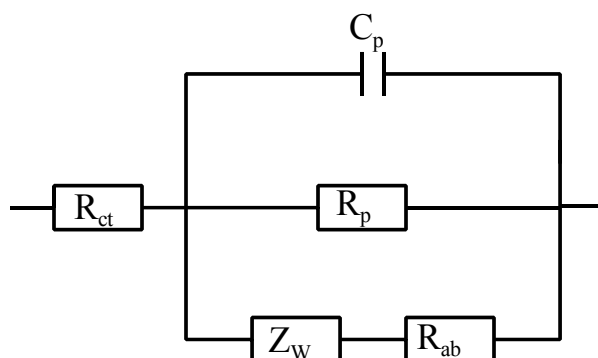
**Figure 5.** Equivalent electrical model of the faradaic impedance for hydrogen absorption and evolution.

A case of finite diffusion length and transmissive boundary conditions has also been considered in the literature.[42,43] It represents the case of a metallic membrane where, at one side $H^+$ is reduced and H enters the metal and on the other side H is oxidized. The only difference is that in the mass-transfer impedance function coth is replaced by tanh, see also Part 1, Section III.6.

When the parameter $\sqrt{j\omega/D_H}\, l$ decreases, that is when frequency is very low or the layer thickness is small, $\coth(x)/x \approx 1/x^2 + 1/3$, and $\hat{Z}_W$, Eq. (88), then simplifies to:

$$\hat{Z}_W = \frac{\sigma' l}{3D_H} - j\frac{\sigma'}{\omega l} = R_W - j\frac{1}{\omega C_W} \tag{89}$$

with $R_W = \sigma' l/(3D_H)$, $C_W = l/\sigma'$, and the Warburg impedance represents a simple $R_W - C_W$ connection in series (see Eq. (100), Part I) in the equivalent circuit.

Figure 6 presents an example of the complex plane plots obtained in the absence and in the presence of the hydrogen evolution reaction. In the case of hydrogen evolution only (without absorption), two semicircles (continuous line), related to two time constants, $R_{ct}$-$C_{dl}$ and $R_p$-$C_p$, are observed. In the presence of H absorption (dashed line), three semicircles, corresponding to the charge-transfer resistance, $R_{ct}$, absorption resistance, $R_{ab}$, and adsorption resistance, $R_p$, together with H diffusion effects (part of a straight line at 45°) are observable. When the absorption reaction is very fast the semi-circle corresponding to H absorption disappears (dot-dashed line). Finally, when the absorption
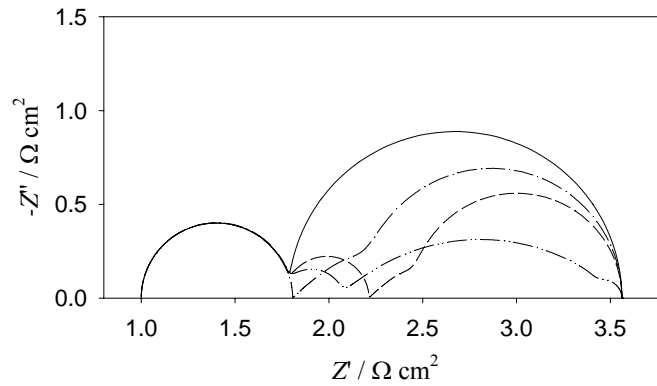


**Figure 6.** Complex plane plots for the hydrogen adsorption, absorption and evolution reaction in the case of the reflecting surface; $k_1 = 2\ 10^{-7}$, $k_{-1} = 2\ 10^{-6}$, $k_2 = 2\ 10^{-6}$ mol s$^{-1}$ cm$^{-2}$, $\eta = -0.05$ V, $l = 0.02$ cm, $D_H = 10^{-7}$ cm$^2$ s$^{-1}$, $C_{dl} = 20$ µF cm$^{-2}$, $\sigma_1 = 210$ µC cm$^{-2}$, $\sigma_X = 10^4$ F cm$^{-3}$, $R_{ct} = 0.801$ Ω cm$^2$, $R_p = 1.76$ Ω cm$^2$, $C_p = 2.78\ 10^{-3}$ F cm$^{-2}$; Continuous line (--): no hydrogen absorption, ($k_4 = k_{-4} = 0$), Dashed line (- -): $k_4 = 2\ 10^{-6}$, $k_{-4} = 10^{-6}$ mol cm$^{-2}$ s$^{-1}$, $R_{ab} = 0.537$ Ω cm$^2$, $\sigma' = 7.12\ 10^{-6}$ Ω cm$^3$ s$^{-1}$; Dot-dashed line ($-\cdot-$): $k_4 = 2\ 10^{-4}$, $k_{-4} = 10^{-4}$ mol cm$^{-2}$ s$^{-1}$, $R_{ab} = 5.37\ 10^{-3}$ Ω cm$^2$, $\sigma' = 7.12\ 10^{-6}$ Ω cm$^3$ s$^{-1}$; Dot-dot-dashed line ($-\cdot\cdot-$): $k_4 = 2\ 10^{-4}$, $k_{-4} = 10^{-6}$ mol cm$^{-2}$ s$^{-1}$, $R_{ab} = 0.295$ Ω cm$^2$, $\sigma' = 2.15\ 10^{-4}$ Ω cm$^3$ s$^{-1}$.

reaction is much faster than desorption (dot-dot-dashed line), a depressed semicircle is observed.

In the presence of hydrogen evolution, the faradaic impedance changes from $R_{ct}$ (at $\omega \to \infty$) to $R_{ct} + R_p$ at $\omega \to 0$. This means that the total impedance varies from $R_s$ at $\omega \to \infty$ to $R_s + R_{ct} + R_p$ at $\omega = 0$. This is because, at low frequencies, the mass-transfer impedance becomes infinite and the equivalent circuit reduces to that applicable for the HER.

## 2. Absorption of the UPD hydrogen

For the case when the Volmer reaction is followed by the hydrogen absorption (e.g. in the case of the hydrogen UPD followed by H absorption or reaction at positive overpotentials), the circuit becomes simplified because $B = -AC$, $R_p^{-1} = 0$ and $R_p$ is infinite. In this case, the faradaic impedance is described by:

$$\hat{Z}_f = R_{ct} + \cfrac{1}{j\omega C_p + \cfrac{1}{R_{ab} + \sigma' \cfrac{\coth\left(\sqrt{\dfrac{j\omega}{D_H}}\, l\right)}{\sqrt{j\omega D_H}}}}$$

$$= R_{ct} + \cfrac{1}{j\omega C_p + \cfrac{1}{R_{ab} + \hat{Z}_W}}$$

(90)

where $C_p = A/C$, $R_{ab} = C/AD = 1/C_p D$ and $\sigma'$ reduces to: $\sigma' = CE/AD = E/C_p D$. Comparison of the complex plane plots for hydrogen UPD, and hydrogen UPD followed by H absorption, is illustrated in Figure 7. The first semi-circle corresponds to the charge-transfer resistance, $R_{ct}$. An additional semi-circle, related to $R_{ab}$, is observed in the case of H absorption. It is followed by the feature corresponding to finite-length diffusion, i.e. a line at 45° and a
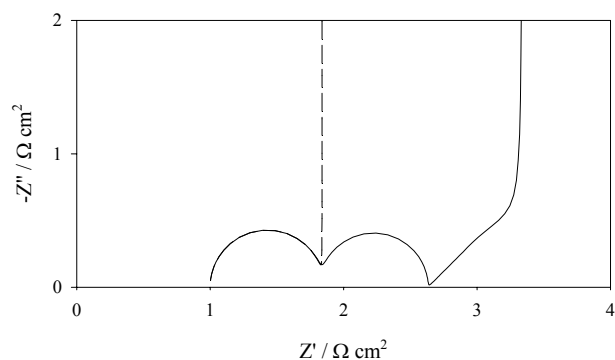
**Figure 7.** Complex plane plots for the hydrogen UPD (dashed line) and UPD followed by hydrogen absorption (continuous line) in the conditions of reflecting boundary. Parameters: $k_1 = 2 \ 10^{-7}$, $k_{-1} = 2 \ 10^{-6}$, $k_4 = 2 \ 10^{-6}$, $k_{-4} = 10^{-6}$ mol cm$^{-2}$ s$^{-1}$, $l = 0.02$ cm, $\eta = -0.05$ V vs. adsorption maximum, other parameters as in Figure 6. Calculated parameters: $R_{ct} = 0.855 \ \Omega$ cm$^2$, $R_{ab} = 0.776 \ \Omega$ cm$^2$, $C_p = 1.98 \ 10^{-3}$ F cm$^{-2}$.

capacitive line (vertical line). In the absence of the absorption reaction the semi-circle connected with $R_{ct}$ is followed by one arising from a pseudocapacitance.

Comparison of the complex plane plots in the case of the H adsorption/absorption processes, for the case of reflecting and transmissive conditions is shown in Figure 8. For the case of transmissive conditions, it was assumed that the concentration of adsorbed H at $x = l$ is equal to zero, i.e. the applied potential is so positive that all the H diffusing across the membrane is immediately oxidized.

Further simplification is achieved when the resistance of H absorption is fast. In this case, $R_{ab} = 0$, reaction (68) is in equilibrium and $\sigma'$ reduces to:
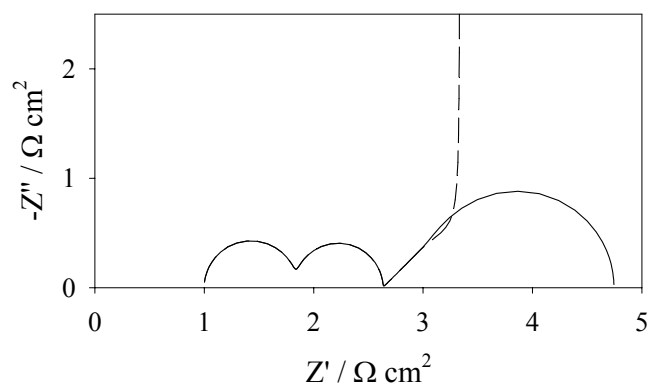
**Figure 8.** Complex plane plots for the hydrogen adsorption/absorption reaction obtained in the case of reflective (dashed line) and transmissive (continuous line) conditions; parameters as in Figure 7.

$$\sigma' = \frac{\sigma_1}{\sigma_x C_p K_4}\left[\Theta\left(K_4 - 1\right) + 1\right]^2 \tag{91}$$

where $K_4 = k_4/k_{-4}$ which reduces to $\sigma' = \sigma_1 \Theta^2 K_4 / \sigma_x$ for large values of the equilibrium constant, $K_4$. An example of the complex plane plot obtained for such a case is shown in Figure 9.

### 3. Spherical diffusion

Very often H absorption is studied on $AB_5$ or $AB_2$ type alloy electrode materials. They form powders for which a finite-length spherical diffusion tratment must be used.[48-50] In such cases, the H diffusion equation (70) must be modified into:
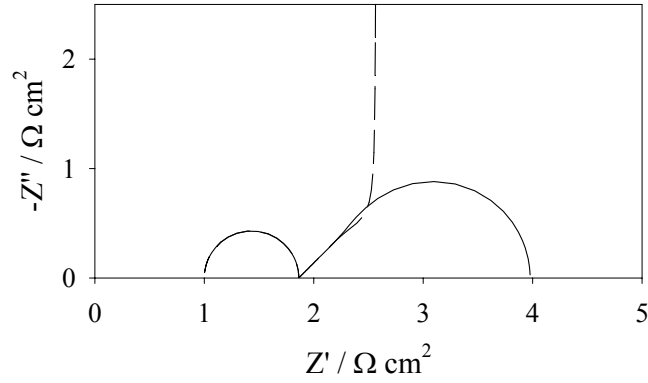
**Figure 9.** Complex plane plots for the hydrogen adsorption/absorption reaction in the case of reflective (dashed line) and transmissive (continuous line) conditions and fast absorption, $k_4 = 2 \ 10^{-4}$, $k_{-4} = 10^{-4}$ mol cm$^{-2}$ s$^{-1}$, other parameters as in Figure 8.

$$\frac{\partial X}{\partial t} = D_{\mathrm{H}} \left[ \frac{\partial^2 X}{\partial r^2} + \frac{2}{r} \frac{\partial X}{\partial r} \right] \tag{92}$$

This equation may be solved using the substitution: $u = X\,r$. For the oscillating concentration, $\tilde{X}$,

$$\frac{\partial \tilde{u}}{\partial t} = D_{\mathrm{H}} \frac{\partial^2 \tilde{u}}{\partial x^2} \quad \text{or} \quad j\omega\tilde{u} = D_{\mathrm{H}} \frac{d^2 \tilde{u}}{dr^2} \tag{93}$$

is obtained for the following boundary conditions:

$$r = r_0 \qquad \tilde{J}_H = -D_H \frac{\sigma_x}{F} \frac{d\tilde{X}}{dr}\bigg|_{r_0}$$  (94)

$$r = 0 \qquad \tilde{u} = 0$$

The solution of Eq. (94) is:

$$\tilde{u} = A e^{sr} + B e^{-sr} \qquad s = \sqrt{\frac{j\omega}{D_H}}$$  (95)

The second boundary condition gives $A = -B$. Application of the first boundary condition to the solution for $\tilde{X}$ gives:

$$\tilde{X} = \frac{A}{r}\left(e^{sr} - e^{-sr}\right)$$

$$\frac{d\tilde{X}}{dr}\bigg|_{r=r_0} = -\frac{2A}{r_0^2}\sinh(sr_0) + \frac{2As}{r_0}\cosh(sr_0) =$$

$$= -\frac{2A}{r_o^2}\left[r_0 s \cosh(sr_0) - \sinh(sr_0)\right] = -\frac{F}{\sigma_x D_H}\tilde{J}_H$$  (96)

$$A = \frac{F r_0^2 \tilde{J}_H}{2\sigma_x D_H}\left[r_0 s \cosh(sr_0) - \sinh(sr_0)\right]^{-1}$$

$$\tilde{X}_0 = \frac{F r_0 \tilde{J}_H}{D_H \sigma_x} \frac{1}{sr_0 \coth(sr_0) - 1}$$

Then the flux at the electrode surface is given by:

$$\tilde{J}_H = \frac{\sigma_x}{F}\tilde{X}_0\left[\sqrt{j\omega D_H}\coth\left(\sqrt{\frac{j\omega}{D_H}}r_0\right) - \frac{D_H}{r_0}\right]$$  (97)

and the Warburg impedance in Eq. (87) is:

$$\hat{Z}_W = \frac{\sigma'}{\sqrt{j\omega D_{\mathrm{H}}}\coth\left(\sqrt{\dfrac{j\omega}{D_{\mathrm{H}}}}r_0\right) - \dfrac{D_{\mathrm{H}}}{r_0}} = \frac{\sigma'}{\dfrac{D_{\mathrm{H}}}{r_0}\left[(sr_0)\coth(sr_0) - 1\right]} \qquad (98)$$

Spherical diffusion changes the shape of the diffusional part of the impedance behavior. Comparison of the results for linear and spherical diffusion is illustrated in Figure 11.

It is interesting to compare relative contributions of $Z_W$, $Z_p$ (equal to the parallel connection of $C_P$ and $Z_W$) to the total impedance, $Z_{\mathrm{tot}}$. Such a comparison is presented in Figure 11. When the parameter $sr_0 = \sqrt{j\omega/D_{\mathrm{H}}}\,r_0$ is small, that is when frequency is sufficiently low or the particle radius is small, $1/(x\coth(x)-1)$ simplifies to $3/x^2+1/5$ and $\hat{Z}_W$, Eq. (98), then becomes simplified to:

$$\hat{Z}_W = R_w + \frac{1}{j\omega C_W} = \frac{\sigma' r_0}{5 D_{\mathrm{H}}} + \frac{1}{j\omega}\frac{3\sigma'}{r_0} \qquad (99)$$

This represents a $R_{\mathrm{W}}$-$C_{\mathrm{W}}$ behavior of the Warburg impedance, with $R_W = \sigma' r_0/5D_{\mathrm{H}}$ and $C_w = r_0/3\sigma'$. Such behavior is different from that observed for thin, planar reflective electrodes, Eq. (89), where $Z_{\mathrm{W}}$ reduces to $R_W - C_W$ at low frequencies.

Absorption of H has been studied at Pd both in transmissive[42,43] and reflective[46,47,51,52] conditions, and at various hydrogen-absorbing alloys such as: LaNi$_5$,[53-55] mishmetals,[49, 56-58] and at bilayers.[44,59] Not all authors have used the correct equation developed for the H adsorption-absorption process. An example of the impedance curves obtained for a Pd electrode in the case of reflective conditions is shown in Figure 12. It displays features similar to those simulated in Figure 9 or 7. For a very thin Pd layer, no diffusional feature (straight line at 45° in the complex plane plots) was observed. In this case, the Warburg impedance was reduced to a $R_{\underline{\mathrm{W}}}$-$C_{\mathrm{W}}$ connection, Eq. (89).
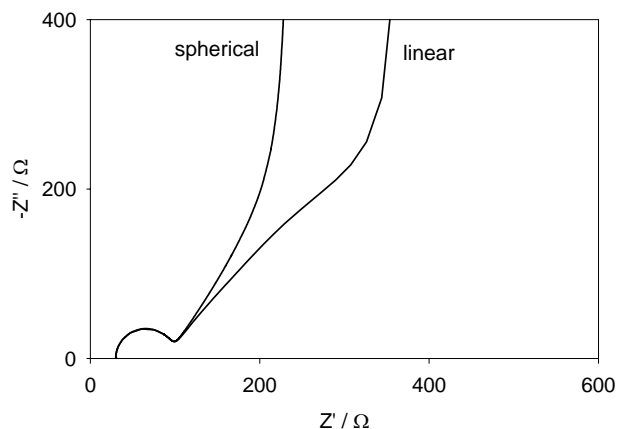
**Figure 10.** Complex plane plots for finite length linear and spherical diffusion. Parameter used: $C_{dl} = 10^{-4}$ F, $C_p = 3 \ 10^{-3}$ F, $\sigma = 0.07 \ \Omega \ s^{-1/2}$, $l = r_0 = 0.005$ cm, $R_{ct} = 70 \ \Omega$, $R_s = 30 \ \Omega$, $R_p = R_{ab} = 0$.

An experimental impedance complex plane plot for the case of transmissive conditions is shown in Figure 13. In such a case, the impedance at low frequencies becomes a real value connected with the transfer of H across the membrane under such conditions.

Hydrogen absorption and phase transitions are accompanied by volume changes leading to a self-induced mechanical stress.[60] These effects were taken into account by Żółtowski[61] in description of the impedance behavior for such conditions.

## 4. Transfer functions approach

Hydrogen absorption in metals may be studied for the conditions of diffusion across a metallic membrane (e.g. Pd, Fe). This process is shown schematically in Figure 14. In this case, using a Devanathan-
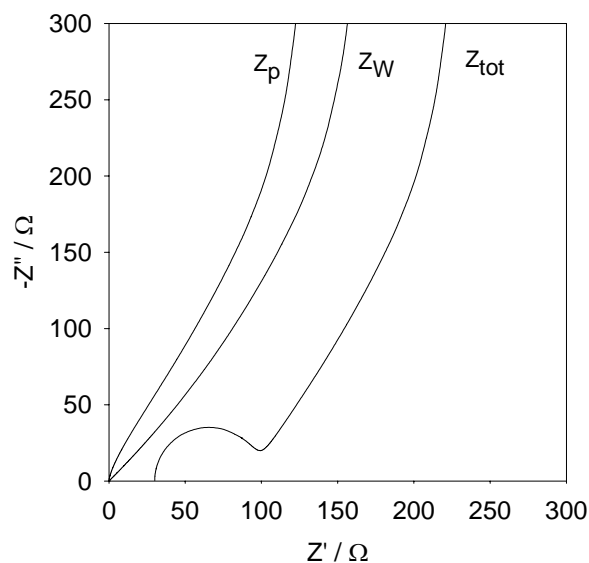
**Figure 11.** Comparison of Warburg impedance, $Z_W$, $Z_p = 1/(j\omega C_p + 1/Z_W)$ and the total impedance, $Z_{tot}$, for a spherical diffusion of hydrogen. parameters as in Figure 10.

Stachurski cell,[62] it is possible to study other complex functions, different from impedance, using the so-called transfer function approach[63-65]. In general, response of the electrical system, $R(t)$, depends on the perturbation, $P(t)$, applied to the system. An equation:

$$R(t) = L\{P(t)\} \tag{100}$$

can be written, where $L$ is an operator characterizing the system. If the system consists of linear elements, the operator $L$ is linear. Electrochemical systems, are, however, fundamentally nonlinear but they may be linearized for conditions of small perturbation, $P(t)$. For an arbitrary applied signal, the output can be related to input by taking
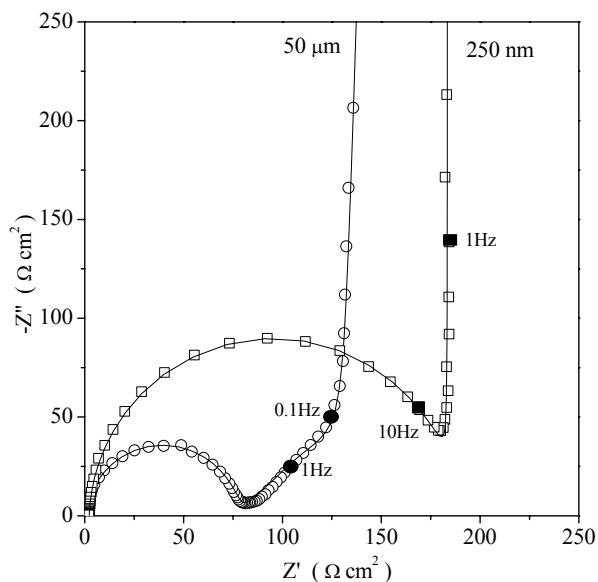
**Figure 12.** Complex plane plots obtained on Pd electrode in 0.1 M $H_2SO_4$ at $\eta_0 = 0.15$ V at a 250 nm Pd film deposited on Au and on 50 μm Pd membrane immersed in the solution in the case of reflective conditions. Points – experimental, lines CNLS approximations.[66]

Laplace transforms of the perturbation and the signal. A transfer function, called the impedance, $Z(s)$, is defined as (see Eq. (6), Part I):

$$Z(s) = \frac{P(s)}{R(s)} = \frac{\mathcal{L}\{E(t)\}}{\mathcal{L}\{i(t)\}} \tag{101}$$

where $\mathcal{L}$ is the Laplace transform operator. The transfer function characterizes response of the system to the applied perturbation. Its knowledge permits prediction of the system response.
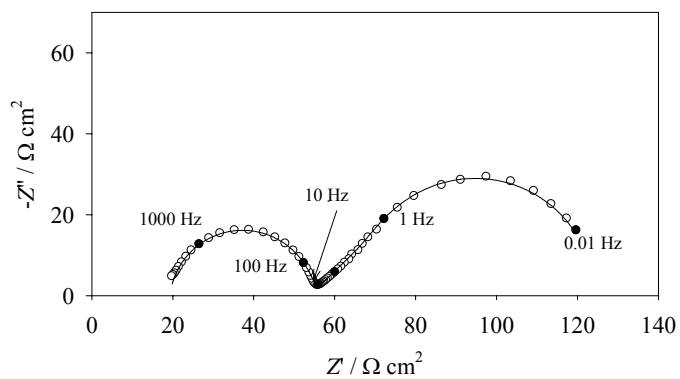
**Figure 13.** Complex plane plots obtained on Pd membrane ($l$ = 50 μm) in the case of transmissive conditions, $\eta_0$ = 90 mV, $\eta_l$ = 280 mV in 0.1 M $H_2SO_4$; points – experimental, line – CNLS approximation.[66]
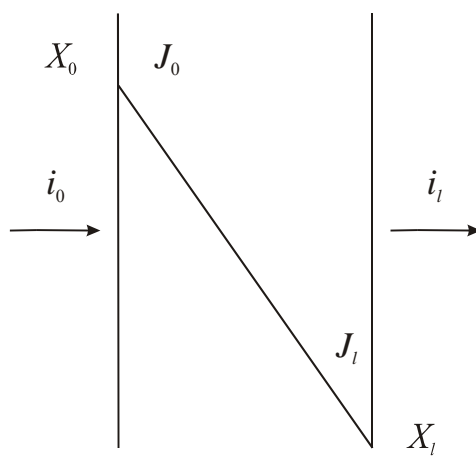


**Figure 14.** Hydrogen transfer across the Pd membrane; reduction current $i_0$, oxidation current $i_l$, hydrogen flux entering $J_0$ and leaving $J_l$ the membrane, $X_0$ and $X_l$ dimensionless concentrations of hydrogen in membrane.

In ac techniques, the perturbation is a periodic function (sin, cos). In order to resolve the problem, one can use the Fourier transform analog of Eq. (100), viz

$$\hat{R}(\omega) = \hat{H}_{R,P}(\omega)\,\hat{P}(\omega) \tag{102}$$

where $\hat{P}(\omega)$ and $\hat{R}(\omega)$ are the Fourier transforms of the perturbation $P(t)$ and the response $R(t)$, and $\hat{H}_{R,P}(\omega)$ is the transfer function relating response to the perturbation.[65-68] In the particular case when $\hat{P}(\omega) = \tilde{E}(\omega)$ and $\hat{R}(\omega) = \tilde{i}(\omega)$, transfer function $\hat{H}_{R,P}(\omega) = \hat{R}(\omega)/\hat{P}(\omega) = \tilde{i}(\omega)/\tilde{E}(\omega) = \hat{Y}(\omega)$, called the admittance. Of course, the inverse of this function is the impedance. In general, various transfer functions may be defined, e.g. mass response of conducting-polymer, $\tilde{m}(\omega)$, to the applied ac perturbation, $\tilde{E}(\omega)$, the so-called electrogravimetric transfer function: $\tilde{m}(\omega)/\tilde{E}(\omega)$.[69,70] Other transfer functions include the electro-optical transfer function i.e. the transfer function for the relation between between current and reflectance, the electrocoulometric transfer function, i.e. transfer function between ring and disk currents, and electrohydrodynamical impedance where the perturbation is a modulation of the angular velocity of the rotating disk electrode, and also magnetohydrodynamical impedance,[68] etc.

In the case of a metallic membrane, "ordinary" transfer function relating current $\tilde{i}$ to the applied potential $\tilde{E}$ is an admittance $\tilde{i}_0 = \hat{Y}_{j_0,E_0}\tilde{E}_0$, where index 0 denotes parameters at $x = 0$, i.e. at the entry side of a membrane. However, one can also measure H transfer across the membrane, i.e. currents measured at both sides of the membrane $\tilde{i}_l = \hat{H}_{i_l,i_0}\tilde{i}_0$ where index $l$ indicates the exit side. It should be noticed that $\hat{H}_{i_l,i_0}$ is dimensionless. Another possible transfer function is: $\tilde{i}_l = \hat{H}_{i_l,E_0}\tilde{E}_0$ which has the units of impedance and characterizes the current measured on the exit side in a response to a sinusoidal potential perturbation on the entry side. Also there is $\hat{H}_{E_l,E_0}$ which is a potentiometric transfer function describing variations of the potential at the exit side ($i_l$ equals to zero) under perturbation at the entry side. It

should be stressed that $\hat{H}_{E_l,i_l}$ is always zero or infinity depending on the constant-potential or constant-current conditions. The above defined transfer functions may be measured using a frequency response analyzer.

We can now determine transfer functions for the case of H permeation. Let it be supposed that on the entry side a sinusoidal perturbation is superimposed on a dc potential and, at the exit side, the applied potential is sufficiently positive that H arriving from across the membrane is immediately oxidized, Figure 14. In this case we have to solve the diffusion equation, Eq. (72), with the following boundary conditions:

$$
\begin{aligned}
x &= 0 && \tilde{X} = \tilde{X}_0 \\
x &= l && \tilde{X} = 0
\end{aligned}
\tag{103}
$$

The solution is:

$$
\tilde{X} = \tilde{X}_0 \frac{\sinh\left[s(l-x)\right]}{\sinh(sl)}
\tag{104}
$$

The flux of H in the membrane is given by:

$$
\tilde{J}(x) = -D_H \frac{\sigma_X}{F}\left(\frac{d\tilde{X}}{dx}\right) = D_H \frac{\sigma_X}{F} s\tilde{X}_0 \frac{\cosh\left[s(l-x)\right]}{\sinh(sl)}
\tag{105}
$$

The fluxes at $x = 0$ and $x = l$ are:

$$
\begin{aligned}
\tilde{J}_0 &= \tilde{J}_H = \frac{\sigma_X}{F}\sqrt{j\omega D_H}\,\tilde{X}_0 \coth(sl) \\
\tilde{J}_l &= \frac{\sigma_X}{F}\sqrt{j\omega D_H}\,\tilde{X}_0 \frac{1}{\sinh(sl)}
\end{aligned}
\tag{106}
$$

Hydrogen (H) concentrations and fluxes at $x = 0$ and $x = l$ are related by the following equation:[64]

$$\begin{bmatrix} \tilde{X}_0 \\ \tilde{J}_0 \end{bmatrix} = \begin{bmatrix} \cosh(sl) & \sinh(sl)/sD_H \\ sD_H \sinh(sl) & \cosh(sl) \end{bmatrix} \begin{bmatrix} \tilde{X}_l \\ \tilde{J}_l \end{bmatrix} \tag{107}$$

The transfer function for fluxes, calculated from Eq. (106), is:

$$\hat{H}_{J_l,J_0} = \frac{\tilde{J}_l}{\tilde{J}_0} = \frac{1}{\cosh(sl)} \tag{108}$$

This function may be separated into a real and imaginary part and a new expression is obtained:

$$\hat{H}_{J_l,J_0} = 2\frac{\cos(\zeta)\cosh(\zeta) - j\sin(\zeta)\sinh(\zeta)}{\cos(2\zeta) + \cosh(2\zeta)} \tag{109}$$

where $\zeta = \sqrt{\omega/2D_H}\, l = \mathrm{Re}(sl)$. The transfer function $\hat{H}_{J_l,J_0}$ is dimensionless and normalized.

A complex plane plot illustrating the flux transfer function is shown in Figure 15 and the dependence of the real and imaginary parts of this transfer function as a function of the logarithm of the frequency is displayed in Figure 16.

However, the H flux $J_0$ is not measurable; only the currents on both sides of the membrane may be determined; the total current on the entry side is $i_{tot} = FJ_{tot}$ and that at the exit side is $\tilde{i}_l = F\tilde{J}_l$ (if the only reaction at $x = l$ is that of H oxidation). The total current flowing to the membrane on the entry side consists of that for double-layer charging, $\tilde{i}_{dl}$, and the faradaic, $\tilde{i}_f$, currents: $\tilde{i}_{tot} = \tilde{i}_{dl} + \tilde{i}_f$. Then, from purely electrical analysis of the equivalent circuit:
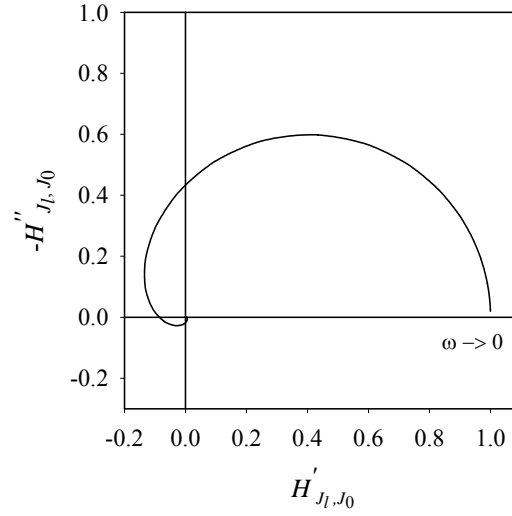
**Figure 15.** The transfer function $\hat{H}_{J_l,J_0}$ complex plane plot for H permeation across the membrane, $l = 10$ μm in thickness, assuming $D_H = 10^{-7}$ cm$^2$ s$^{-1}$.

$$\frac{\tilde{i}_f}{\tilde{i}_{tot}} = \frac{\dfrac{1}{j\omega C_{dl}}}{\dfrac{1}{j\omega C_{dl}} + \hat{Z}_f} = \frac{1}{1 + j\omega C_{dl}\hat{Z}_f} \qquad (110)$$

In the same way one can find the ratio of the current flowing through the $R_{ab}$-$\hat{Z}_W$ branch, Figure 5, i.e. the current entering the membrane, to the faradaic current, $\tilde{i}_0/\tilde{i}_f$ :
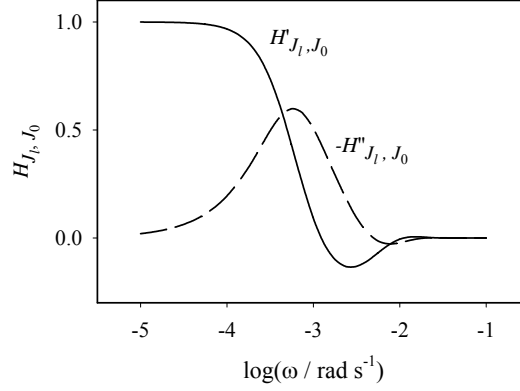
**Figure 16.** Real and imaginary parts of the transfer function $\hat{H}_{J_l, J_0}$ as functions of the logarithm of the angular frequency; parameters as in Figure 15.

$$\frac{\tilde{i}_0}{\tilde{i}_f} = \frac{\dfrac{1}{j\omega C_p}}{\dfrac{1}{j\omega C_p} + R_{ab} + \hat{Z}_W} = \frac{1}{1 + j\omega C_p \left( R_{ab} + \hat{Z}_W \right)}$$

$$= \frac{1}{1 + j\omega \left[ \dfrac{1}{D} + \dfrac{E}{D} \dfrac{\tanh(sl)}{\sqrt{j\omega D_H}} \right]}$$

$\qquad\qquad\qquad\qquad\qquad\qquad\qquad\qquad$ (111)

where $\hat{Z}_W = (CE / AD)\tanh(sl)/\sqrt{j\omega D_H}$  Taking into account Eqs. (108), (110) and (111) the transfer function for currents can be obtained as:

$$\frac{\tilde{i}_l}{\tilde{i}_{tot}} = -\frac{1}{\cosh(sl)\left(1 + j\omega C_{dl}\hat{Z}_f\right)\left[1 + j\omega C_p \left( R_{ab} + \hat{Z}_W \right)\right]}$$

$\qquad\qquad\qquad\qquad\qquad\qquad\qquad\qquad$ (112)
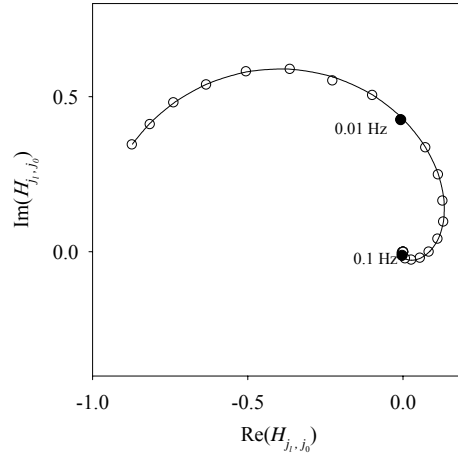
**Figure 17.** Complex plane plot of the experimental transfer functions $\hat{H}_{i_l, i_0}$ at $\eta_0 = 90$ mV and $\eta_l = 480$ mV for hydrogen transfer across the Pd membrane, $l = 50$ μm, in 0.1 M $H_2SO_4$, points – experimental, line - approximation.[66]

An example of the current transfer function for H transfer across a Pd membrane is shown in Figure 17. Because the frequencies studied were below 0.2 Hz, only the first term in Eq. (112), containing $\cosh(sl)$ was important, that is Eq. (108) was sufficient to approximate the results.

In a similar way it is possible to determine the transfer function of the exit current to the applied potential, $\tilde{i}_l / \tilde{\eta}$. It has the dimensions of admittance and can be obtained from Eq. (112) as:

$$\frac{\tilde{i}_l}{\tilde{i}_{tot}} = \frac{\tilde{i}_l / \tilde{\eta}}{\tilde{i}_{tot} / \tilde{\eta}} = \frac{\tilde{i}_l / \tilde{\eta}}{1/\hat{Z}_{tot}} \tag{113}$$

$$\frac{\tilde{i}_l}{\tilde{\eta}} = -\frac{1}{\cosh(sl)\left(1 + j\omega C_{dl}\hat{Z}_f\right)\left[1 + j\omega C_p\left(R_{ab} + \hat{Z}_W\right)\right]\hat{Z}_{tot}}$$

Because the membrane thickness is typically $\geq 20$ μm, only diffusional effects are observed at very low frequencies.

Hydrogen transfer functions have been studied for iron[65, 71] and palladium.[72]

It should be added that intercalation of metal ions into solid matrices, e.g. in Li-ion electrode systems, may be formally described by equations similar to those for electrochemical absorption of H.

## REFERENCES

1. A. Lasia, *Electrochemical Impedance Spectroscopy and its Applications* in *Modern Aspects of Electrochemistry*, vol. 32, R. E. White, B. E. Conway, and J. O'M. Bockris, Eds., Plenum Press, New York, 1999, p. 143.
2. D.A. Harrington, *J. Electroanal. Chem.*, **403** (1996) 11; **449** (1998) 9, 29.
3. D. A. Harrington and P. van den Driessche, *Electrochim. Acta*, **44** (1999) 4321.
4. E. Leiva, *Electrochim. Acta*, **41** (1996) 2185.
5. D. A. Harrington and B. E. Conway, *Electrochim. Acta*, **32** (1987) 1703.
6. A. Lasia, *Polish J. Chem.*, **69** (1995) 639.
7. A. Lasia in *Proceedings of the Symposium on Electrochemistry and Materials Science of Cathodic Hydrogen Absorption and Adsorption*, B.E. Conway and G. Jerkiewicz, Eds., The Electrochemical Society, **94-21**, 1994, p. 261.
8. D. A. Harrington and B.E. Conway, *J. Electroanal. Chem.*, **221** (1987) 1.
9. S. Morin, H. Dumont, and B.E. Conway, *J. Electroanal. Chem.*, **412** (1996) 39.
10. D. A. Harrington, *J. Electroanal. Chem.*, **355** (1993) 21.
11. A. Lasia, *Current Topics Electrochem.*, **2** (1993) 239.
12. E. R. Gonzalez, G. Tremiliosi-Filho, and M. J. de Giz, *Current Topics Electrochem.*, **2** (1993) 167.
13. L. Bai, D. A. Harrington, and B. E. Conway, *Electrochem. Acta*, **32** (1987) 1713.
14. P. Gu, L. Bai, L. Gao, R. Brousseau, and B. E. Conway, *Electrochim. Acta*, **37** (1992) 2145.
15. R. Simpraga, G. Tremiliosi-Filho, S. Y. Qian, and B. E. Conway, *J. Electroanal. Chem.*, **424** (1997) 141.
16. J. Fournier, P. K. Wrona, A. Lasia, R. Lacasse, J.-M. Lalancette, and H. Ménard, *J. Electrochem. Soc.,* **139** (1992) 2372.
17. H. Dumont, P. Los, A. Lasia, and H. Ménard, *J. Appl. Electrochem.,* **23** (1993) 684.

18. H. Dumont, P. Los, L. Brossard, A. Lasia, and H. Ménard, *J. Electrochem. Soc.,* **139** (1992) 2143.
19. Y. Choquette, L. Brossard, A. Lasia, and H. Ménard, *J. Electrochem. Soc*., **137** (1990) 1723.
20. Y. Choquette, L. Brossard, A. Lasia, and H. Ménard, *Electrochim. Acta*, **35** (1990) 1251.
21. A. Lasia and A. Rami, *J. Electroanal. Chem*., **294** (1990) 123.
22. L. Chen and A. Lasia, *J. Electrochem. Soc.,* **138** (1991) 3321.
23. P. Los and A. Lasia, *J. Electroanal. Chem*., **333** (1992) 115.
24. J. J. Borodzinski and A. Lasia, *J. Appl. Electrochem.,* **24** (1994) 1267.
25. R. Karimi Shervedani and A. Lasia, *J. Electrochem. Soc.,* **144** (1997) 511.
26. R. Karimi Shervedani and A. Lasia, *J. Electrochem. Soc.,* **144** (1997) 2652.
27. L. Chen and A. Lasia, *J. Electrochem. Soc.,* **139** (1992) 3214.
28. C. Hitz and A. Lasia, *J. Electroanal. Chem*., **500** (2001) 213.
29. L. Chen and A. Lasia, *J. Electrochem. Soc.,* **140** (1993) 2464.
30. L. Chen and A. Lasia, *J. Electrochem. Soc*., **139** (1992) 3458.
31. A. Rami and A. Lasia, *J. Appl. Electrochem*., **22** (1992) 376.
32. P. Los, A. Rami, and A. Lasia, *J. Appl. Electrochem.,* **23** (1993) 135.
33. P. Los, A. Lasia, L. Brossard, and H. Ménard*, J. Electroanal. Chem.*, **360** (1993) 101.
34. J. Barber, S. Morin, and B. E. Conway, *Proceedings of the Symposium on the Electrochemical Surface Science of Hydrogen Adsorption and Absorption*, G. Jerkiewicz and P. Marcus, Edts., The Electrochemical Society, vol. 97-16, 1997, p. 101.
35. J. H. Barber, S. Morin, and B. E. Conway, *J. Electroanal. Chem.,* **446** (1998) 125.
36. N. M. Marković, B. N. Grgur, and P. N. Ross, *J. Phys. Chem. B*, **101** (1997) 5405.
37. M. J. de Giz, G. Tremiliosi-Filho, and E. R. Gonzalez, *Electrochim. Acta*, **39** (1994) 1775.
38. M. J. de Giz, G. Tremiliosi-Filho, E. R. Gonzalez, S. Srinivasan, and A. J. Appleby, *Int. J.* Hydrogen *Energy*, **20** (1995) 423.
39. E. B. Castro, M. J. de Giz, E. R. Gonzalez, and J. R. Vilche, *Electrochim. Acta*, **42** (1997) 951.
40. N. A. Assunção, M. J. de Giz, G. Tremiliosi-Filho, and E. R. Gonzalez, *J. Electrochem. Soc.,* **144** (1997) 2794.
41. A. Lasia and D. Grégoire, *J. Electrochem. Soc*., **142** (1995) 3393.
42. C. Lim and S.-I. Pyun, *Electrochim. Acta,* **38** (1993) 2645.
43. C. Lim and S.-I. Pyun, *Electrochim. Acta*, **39** (1994) 363.
44. J.S. Chen, R. Durand, and C. Montella, *J. Chim. Phys*., **91** (1994) 383.
45. T.-H. Yang and S.-I. Pyun, *J. Power Sourc*., **62** (1996) 175.
46. T.-H. Yang and S.-I. Pyun, *J. Electroanal. Chem*., **414** (1996) 127.
47. T.-H. Yang and S.-I. Pyun, *Electrochim. Acta*., **41** (1996) 843.
48. C. Wang, *J. Electrochem. Soc*., **145** (1998) 1801.
49. L. O. Valøen, S. Sunde, and R. Tunold, *J. Alloys Comp.,* **253-254** (1997) 656.
50. B.S. Haran, B.N. Popov and R.E. White, *J. Power Sources*, **75** (1998) 56.

51. G. Jorge, R. Durand, R. Faure, and R. Yvari, *J. Less-Common Met.,* **145** (1988) 383.

52. S.-I. Pyun, T.-H. Yang, and C.-S. Kim, *J. Appl. Electrochem*., **26** (1996) 953.

53. P. Agarwal, M.E. Orazem, and A. Hiser in *Proceedings of 19th Symposium on Hydrogen Storage Materials, Batteries and Electrochemistry,* D.A. Corrigan and S. Srinivasan, Eds., Electrochemical Society, Pennington, N.J., 1991, p. 120.

54. T.-H. Yang and S.-I. Pyun, *J. Power Sourc.,* **62** (1996) 175.

55. P. Millet and P. Dantzer, *J. Alloys Comp.*, **253-254** (1997) 542.

56. N. Kuriyama, T. Saki, H. Miyamura, I. Uehara, and T. Iwasaki, *J. Alloys Comp*., **202** (1993) 183.

57. W. Zhang, M. P. S. Kumar, S. Srinivasan, and H.J. Ploehn, *J. Electrochem. Soc.*, **142** (1995) 2935; see also Y. Leng, *ibid.,* **144** (1997) 2941  and W. Zhang and S. Srinivasan, *ibid*., **144** (1997) 2942.

58. X. Gao, J. Liu, S. Ye, D. Song, and Y. Zhang, *J. Alloys Comp.*, **253-254** (1997) 515.

59. Y.-G. Yoon and S.I. Pyun, *Electrochim. Acta*, **40** (1995) 999.

60. B. Baranowski in *Flow, Diffusion, and Rate Processes*, (*Advances of Thermodynamics*, vol. 6), S. Sieniutycz and P. Salamon, Edts., Taylor and Francis, New York, 1992, p. 168.

61. P. Żółtowski, *Electrochim. Acta*, **44** (1999) 4415; *J. Electroanal. Chem.*, **501** (2001) 89.

62. M. A. V. Devanathan and Z. Stachurski, *Proc. Roy. Soc*., **A270** (1962) 90; *J. Electrochem. Soc*., **111** (1964) 619.

63. N. Boes and H. Züchner, *J. Less Common Metals*, **49** (1976) 223.

64. C. Montella, *J. Electroanal. Chem*., **462** (1999) 73; **480** (2000) 150, 166.

65. P. Bruzzoni, R. M. Carranza, J. R. Collet, and E. A. Crespo, *Electrochim. Acta*, **44** (1999) 2693.

66. P.-P. Grand, *PhD Thesis*, Université de Sherbrooke, 2001.

67. C. Gabrielli, M. Keddam, and H. Takenouti, *Electrochim. Acta*, **35** (1990) 1553.

68. C. Gabrielli, B. Tribollet, *J. Electrochem. Soc*., **141** (1994) 1147.

69. C. Gabrielli, M. Keddam, N. Nadi, and H. Perrot, *Electrochim. Acta*, **44** (1999) 2095.

70. C. Gabrielli, M. Keddam, H. Perrot, M.C. Pham, and R. Torresi, *Electrochim. Acta*, **44** (1999) 4217.

71. P. Bruzzoni, R.M. Carranza, J.R. Collet Lacoste, and E.A. Crespo, *Int. J. Hydrogen Energy*, **24** (1999) 1093.

72. P.F. Buckley, J.A. Fagan, and O.C. Searson, *J. Electrochem. Soc*., **147** (2000) 3456.